JOURNAL OF GEOPHYSICAL RESEARCH, VOL. 113, E06S22, doi:10.1029/2007JE002990, 2008

Click Here for Full Article

Meteorites on Mars observed with the Mars Exploration Rovers

C. Schröder,[1] D. S. Rodionov,[2,3] T. J. McCoy,[4] B. L. Jolliff,[5] R. Gellert,[6] L. R. Nittler,[7] W. H. Farrand,[8] J. R. Johnson,[9] S. W. Ruff,[10] J. W. Ashley,[10] D. W. Mittlefehldt,[1] K. E. Herkenhoff,[9] I. Fleischer,[2] A. F. C. Haldemann,[11] G. Klingelhöfer,[2] D. W. Ming,[1] R. V. Morris,[1] P. A. de Souza Jr.,[12] S. W. Squyres,[13] C. Weitz,[14] A. S. Yen,[15] J. Zipfel,[16] and T. Economou[17]

Received 14 August 2007; revised 9 November 2007; accepted 21 December 2007; published 18 April 2008.

[1] Reduced weathering rates due to the lack of liquid water and significantly greater typical surface ages should result in a higher density of meteorites on the surface of Mars compared to Earth. Several meteorites were identified among the rocks investigated during Opportunity's traverse across the sandy Meridiani plains. Heat Shield Rock is a IAB iron meteorite and has been officially recognized as "Meridiani Planum." Barberton is olivine-rich and contains metallic Fe in the form of kamacite, suggesting a meteoritic origin. It is chemically most consistent with a mesosiderite silicate clast. Santa Catarina is a brecciated rock with a chemical and mineralogical composition similar to Barberton. Barberton, Santa Catarina, and cobbles adjacent to Santa Catarina may be part of a strewn field. Spirit observed two probable iron meteorites from its Winter Haven location in the Columbia Hills in Gusev Crater. Chondrites have not been identified to date, which may be a result of their lower strengths and probability to survive impact at current atmospheric pressures. Impact craters directly associated with Heat Shield Rock, Barberton, or Santa Catarina have not been observed, but such craters could have been erased by eolian-driven erosion.

Citation: Schröder, C., et al. (2008), Meteorites on Mars observed with the Mars Exploration Rovers, *J. Geophys. Res.*, *113*, E06S22, doi:10.1029/2007JE002990.

1. Introduction

[2] Mars' cratered landscapes are testimony to ongoing impacts of meteoroids onto its surface. The flux of crater-producing objects is expected to be greater at Mars relative to Earth because of the planet's closer proximity to the asteroid belt [e.g., *Shoemaker*, 1977]. Recent images from orbiting platforms show that hypervelocity impacts persist to the present-day [*Malin et al.*, 2006]. The atmosphere of Mars is thick enough to decelerate meteoroids of small mass sufficiently to survive impact [*Dycus*, 1969]. Weathering and erosion limit the residence time of meteorites on planetary surfaces. On Earth, stony meteorites recovered from Antarctica display the longest terrestrial residence times of up to a few million years [*Scherer et al.*, 1997; *Welten et al.*, 1997], while meteorites in hot desert regions decay at least 1 order of magnitude faster [*Bland et al.*, 1996]. The current climate on Mars is characterized by low temperatures and an extremely limited availability of liquid water. *Bland and Smith* [2000] estimate that meteorite decay due to chemical weathering occurs on a 10^9 year timescale on Mars. On the basis of the larger flux and lower weathering rates, *Bland and Smith* [2000] calculated an average accumulation of ca. 5×10^2 to 5×10^5 meteorites greater than 10 g in mass per square kilometer on Mars, compared to two to three samples per square kilometer in

[1]Astromaterials Research and Exploration Science, NASA Johnson Space Center, Houston, Texas, USA.
[2]Institut für Anorganische und Analytische Chemie, Johannes Gutenberg-Universität, Mainz, Germany.
[3]Also at Space Research Institute IKI, Moscow, Russia.
[4]National Museum of Natural History, Smithsonian Institution, Washington, D. C., USA.
[5]Department of Earth and Planetary Sciences and the McDonnell Center for the Space Sciences, Washington University, St. Louis, Missouri, USA.
[6]Department of Physics, University of Guelph, Guelph, Ontario, Canada.
[7]Department of Terrestrial Magnetism, Carnegie Institution of Washington, Washington, D. C., USA.
[8]Space Science Institute, Boulder, Colorado, USA.
[9]U.S. Geological Survey, Flagstaff, Arizona, USA.
[10]School of Earth and Space Exploration, Arizona State University, Tempe, Arizona, USA.
[11]ESA-ESTEC, Noordwijk, Netherlands.
[12]Vallourec Research Center, Aulnoye-Aymeries, France.
[13]Department of Astronomy, Cornell University, Ithaca, New York, USA.
[14]Planetary Science Institute, Tucson, Arizona, USA.
[15]Jet Propulsion Laboratory, California Institute of Technology, Pasadena, California, USA.
[16]Forschungsinstitut und Naturmuseum Senckenberg, Frankfurt am Main, Germany.
[17]Laboratory for Astrophysics and Space Research, Enrico Fermi Institute, University of Chicago, Chicago, Illinois, USA.

Copyright 2008 by the American Geophysical Union.
0148-0227/08/2007JE002990$09.00

a typical hot desert accumulation site on Earth [*Bland et al.*, 1996]. Therefore both of the NASA Mars Exploration Rovers (MER), Spirit and Opportunity, could be expected to come across meteorites during their journeys. The challenge is to recognize them.

[3] Meteorite finds on the surface of Mars offer another perspective on NASA's "follow-the-water" exploration strategy. The susceptibility of meteorites to rapid alteration processes makes them ideal materials for searching for evidence of climate change on Mars [*Ashley and Wright*, 2004]. Reduced metallic iron, estimated to be present in approximately 88% of all falls on Earth, will oxidize in the presence of water on Mars, even if no additional oxygen is available [e.g., *Gooding et al.*, 1992]. Because of this high reactivity, meteorites found on Mars might exhibit subtle signs of alteration where a Martian basalt, when exposed to the same set of conditions, might not. Both MER rovers are located in near-equatorial latitudes, where surface water exposure under current obliquity cycles is anticipated to be negligible [e.g., *Carr*, 1996], but could be significant within the near-subsurface [*Burr et al.*, 2005]. A single "rusty" meteorite with measurable oxyhydroxides at either location, for example, would therefore be evidence of wetter climatic conditions than exist today. Such a finding would be significant irrespective of meteorite residence time. A lack of oxyhydroxides in meteorites would also offer insight, but questions of residence time become more important in such cases. The difference between irons and stony or stony iron meteorites becomes important here because alteration products may still exist within stony meteorite interiors whereas they may be readily abraded by wind erosion from the surfaces of irons.

[4] At another level of interest, long-lived meteorites on Mars may sample asteroids which have not been sampled on Earth within the last few million years. Because the dynamical characteristics of Mars-crossing objects differ from Earth crossers, the population of impactors that have accumulated on the two objects may differ in initial composition.

[5] Spirit and Opportunity are equipped with the Athena Science Payload [*Squyres et al.*, 2003] consisting of a 0.27 mrad/pixel, multiple filter visible to near-infrared (400 to 1010 nm) Panoramic camera (Pancam) [*Bell et al.*, 2003], a Mini-Thermal Emission Spectrometer (Mini-TES) covering the 5 to 29 μm wavelength region [*Christensen et al.*, 2003], a 30 μm/pixel Microscopic Imager (MI) [*Herkenhoff et al.*, 2003], an Alpha Particle X-ray Spectrometer (APXS) for elemental composition [*Rieder et al.*, 2003], a Mössbauer (MB) spectrometer for determining mineralogy of iron-bearing phases [*Klingelhöfer et al.*, 2003], a set of magnets for attracting dust particles [*Madsen et al.*, 2003], and a Rock Abrasion Tool (RAT) to remove surface contamination and weathering rinds from rock surfaces [*Gorevan et al.*, 2003]. The rovers also carry engineering cameras to support mobility, navigation, science, and placement of the instrument arm [*Maki et al.*, 2003].

[6] Opportunity is exploring the Meridiani Planum region of Mars. The area is characterized by sulfate-rich bedrock largely covered by eolian basaltic sand and lag deposit of hematite-rich spherules [*Squyres et al.*, 2004, 2006a, 2006b]. The basaltic sand cover is typically about 1 m thick; wind deflation exposes bedrock in places and exhumes the hematite spherules which make up the lag deposit [*Soderblom et al.*, 2004]. On Earth, increased accumulations of meteorites are found in areas where wind deflation has removed eolian sand covers [*Zolensky et al.*, 1990]. On the basis of the Ni contents of Martian soil samples and certain sedimentary rocks, *Yen et al.* [2006] estimated an average of 1% to 3% contamination from meteoritic debris.

[7] Numerous rock fragments are also scattered across the surface of Meridiani Planum. These rock fragments, though of diverse origin and composition, seem to be impact-related to some extent. They appear to cluster in troughs between ripples on the plains, and are notably abundant on rocky surfaces in and around impact craters [*Jolliff et al.*, 2006]. During daily rover operations, the MER Science Team refers to any rock larger than 1 cm as a cobble. In this article we will refer to each rock as a pebble, cobble, or boulder according to its diameter. A pebble, in this respect, ranges from 4 mm to 64 mm according to the Krumbein ϕ scale [*Krumbein and Sloss*, 1963].

[8] An approximately 40 cm $\times$ 20 cm isolated boulder, Bounce Rock, is the first rock investigated in situ on the surface of Mars whose chemical and mineralogical composition matches that of basaltic shergottites, a subgroup of more than 30 meteorites whose origin has been interpreted to be Mars. Bounce Rock is particularly similar in composition to lithology B of the meteorite EETA79001 [*Rodionov et al.*, 2004; *Zipfel et al.*, 2004]. The distinct characteristics of Bounce Rock, together with its isolated occurrence, suggest that it is not locally derived. A possible source is a relatively fresh 25 km crater located 75 km southwest of Opportunity's landing site, whose ejecta lie atop the hematite-bearing plains [*Squyres et al.*, 2004].

[9] The pebble FigTree Barberton2 (hereafter referred to as Barberton), discovered at the rim of Endurance crater, and the boulder Heat Shield Rock, discovered south of Endurance Cater, were interpreted as a stony meteorite and an iron meteorite, respectively [*Schröder et al.*, 2006; *Rodionov et al.*, 2005]. Heat Shield Rock is officially recognized as a meteorite with the name "Meridiani Planum" [*Connolly et al.*, 2006]. We will use Heat Shield Rock throughout this article, however, in order to avoid confusion with the location name of Opportunity's landing site. The cobble Santa Catarina discovered at the rim of Victoria crater shows similarities to Barberton. These three rocks will be described in detail in the next chapters. Their location along Opportunity's traverse is shown in Figure 1. Other potential meteorites, also from the Spirit landing site in Gusev Crater, which were not investigated by the full rover payload are described thereafter, followed by a discussion of the general conclusions that can be drawn from this data set.

[10] The place names used in this paper for landforms, rocks, and soils have not been approved by the International Astronomical Union and are meant to be informal and convenient ways to remember features (e.g., an

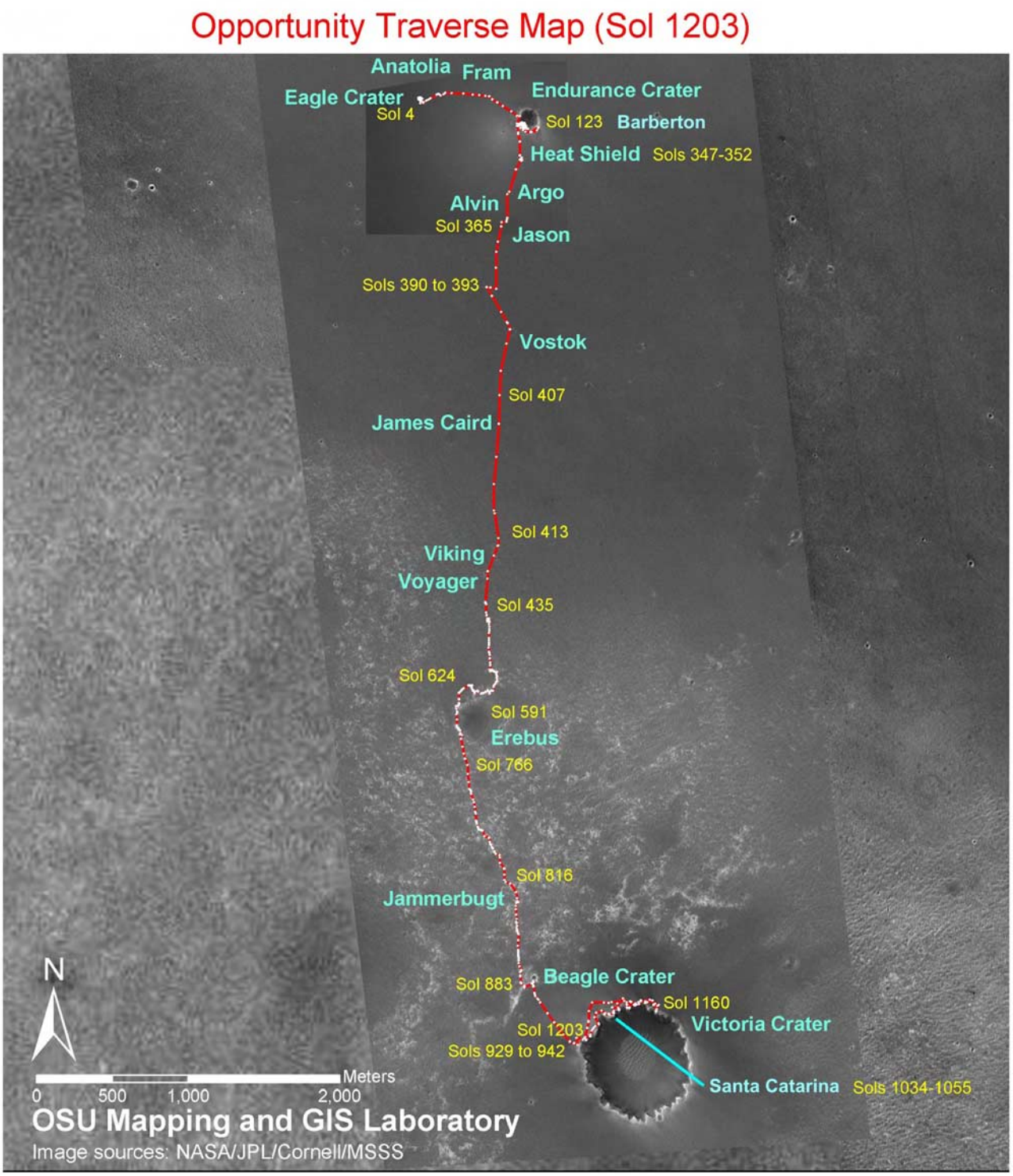

Figure 1. Opportunity traverse map showing large impact craters and the location of Barberton, probably a stony meteorite at the rim of Endurance crater; Heat Shield Rock, an iron meteorite discovered close to Opportunity's heat shield south of Endurance; Santa Catarina on the rim of Victoria crater, similar in composition to Barberton.

outcrop or eolian bed form) and targets (e.g., specific location on a feature for which in situ measurements were acquired). Similarities between the feature and/or target names of rocks discussed as potential meteorites here and the names of actual meteorites in collections on Earth are unintended. In the case that any of the rocks discussed here will be officially recognized as meteorites, we suggest following the example of renaming Heat Shield

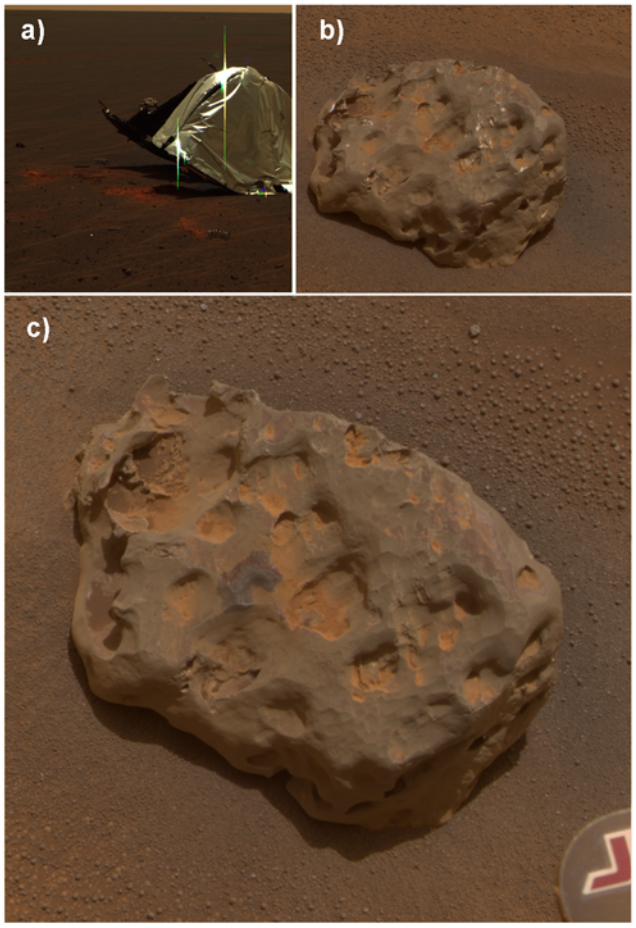

Figure 2. Heat Shield Rock, (a) as first seen close to Opportunity's heat shield (http://marswatch.astro.cornell.edu/pancam_instrument/images/False/Sol335B_P2364_1_False_L257_pos_1.jpg); (b) in a Pancam approximate true color close-up view, showing its pitted surface and high reflectance (http://marswatch.astro.cornell.edu/pancam_instrument/images/True/Sol346B_P2591_1_True_RAD.jpg); (c) the RAT-brushed spot near the center of the rock indicating the area investigated in detail by the remaining IDD instruments (http://marswatch.astro.cornell.edu/pancam_instrument/images/True/Sol352B_P2596_1_True_RAD.jpg). Heat Shield Rock measures 31 cm in its longest dimension.

Rock after the location of the find, i.e., Meridiani Planum, adding a counter where necessary.

2. Heat Shield Rock

[11] Driving south from Endurance crater, Opportunity stopped to investigate the heat shield that had been dropped during the lander's descent to the surface. Heat Shield Rock was found just several meters from the heat shield (Figure 2a). Its maximum dimension is 31 cm. It was first identified as an interesting target on the basis of its unusual appearance in Pancam images, which show a highly pitted surface that is gray in tone with quasi-specular highlights (Figure 2b). Mini-TES observed Heat Shield Rock from two different standoff positions, providing the first clues to its composition. The spectra revealed features that are nearly indistinguishable from those of the Martian atmosphere although at reduced contrast, indicating that the rock is highly reflective at mid-infrared wavelengths. *Ruff et al.* [2008] demonstrated that the spectrum of Heat Shield Rock resembles a gray body with emissivity of ~0.3, a characteristic of metals and consistent with an iron meteorite. Photometric studies of Heat Shield Rock [*Johnson et al.*, 2006] show that it is one of the most forward scattering materials observed by Opportunity, also consistent with a smooth, metallic surface. The surface pits are interpreted as regmaglypts developed by ablation during the descent through the Martian atmosphere. Heat Shield Rock was subsequently investigated with the IDD instruments on both "as is" and RAT-brushed surface targets between sols 347 and 352. No attempt was made to grind the rock because laboratory tests using an engineering model of the RAT on an iron meteorite sample suggested abrading Heat Shield Rock would have led to rapid and substantial bit wear.

2.1. Classification

[12] The APXS-derived bulk elemental composition of Heat Shield Rock is 93% Fe, 7% Ni, ~300 ppm Ge, and <100 ppm Ga (R. Gellert et al., In situ chemistry along the traverse of Opportunity at Meridiani Planum: Sulfate-rich outcrops, iron rich spherules, global soils and various erratics, manuscript in preparation, 2008). Mössbauer spectra show 94% of the Fe in a metal phase. On the basis of the Fe/Ni ratio, this phase was assigned to kamacite, α-(Fe,Ni), by *Morris et al.* [2006]. Small amounts of taenite, γ-(Fe,Ni), are generally present in iron meteorites with 7% bulk Ni, but would be below the MB detection limit within the available counting statistics and the relatively high concentration of other Fe-bearing phases. Heat Shield Rock is classified as a IAB complex iron meteorite based on its Ni and Ge contents (Figure 3). It has acquired official meteorite status with the name "Meridiani Planum" [*Connolly et al.*, 2006].

2.2. Surface Coating

[13] Figure 4a shows a false-color Pancam image of Heat Shield Rock after it was brushed by the RAT. Pancam spectra of bright dust and darker soil that collected in small pits on the surface are typical of materials containing variable amounts of air fall-deposited dust and basaltic soil. The 535 nm band depths of dust/coatings in the pits of Heat Shield Rock are elevated compared to windblown soil, indicating a somewhat greater level of ferric oxide crystallinity in those materials.

[14] Portions of the surface appear coated with a material more purple in the false-color image compared to the majority of the surface and likely represent more oxidized portions of the rock surface as evidenced by the deeper 535 nm band. Such color variations in the brushed and unbrushed portions of the rock are also evident in a MI mosaic colorized with Pancam data (Figure 4b). The brushed, uncoated material appears "blue" in the false-color images and exhibits a spectrum quite similar to laboratory spectra of the Canyon Diablo IAB meteorite, where differences in brightness and spectral slope may be related to differences in surface roughness and/or nickel

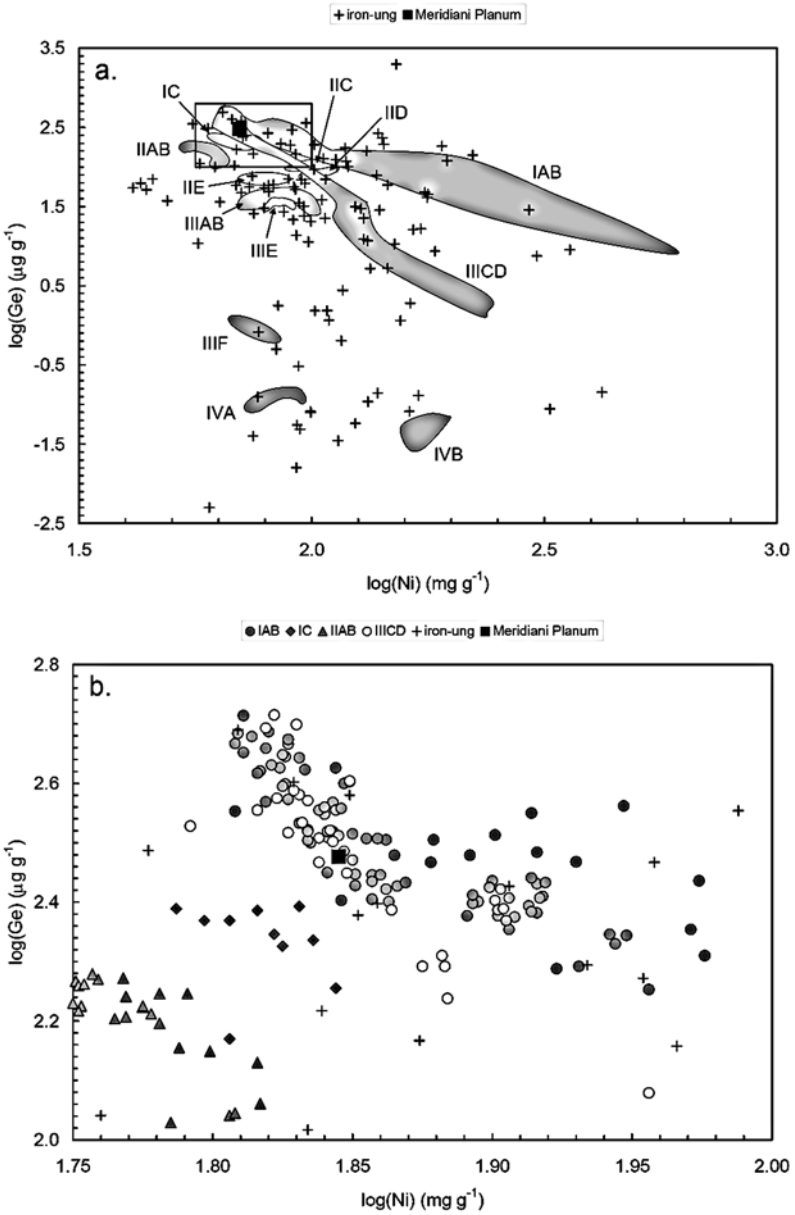

Figure 3. The plot shows log Ge versus log Ni for meteorite Meridiani Planum (Heat Shield Rock) compared to iron meteorites. (a) All iron meteorites show a wide range in Ge content and more limited Ni contents. Meridiani Planum plots within the region occupied by IAB and IIICD irons. Individual ungrouped irons and fields for the 12 iron meteorite groups are shown. Box shows region expanded as b. (b) Meridiani Planum has Ge-Ni characteristics within the ranges of Ni-poor IAB and IIICD irons. Iron meteorite data are averaged from all available analyses from the Wasson group at UCLA [*Choi et al.*, 1995; *Esbensen et al.*, 1982; *Kracher et al.*, 1980; *Malvin et al.*, 1984; *Rasmussen et al.*, 1984; *Schaudy et al.*, 1972; *Scott*, 1978; *Scott and Wasson*, 1976; *Scott et al.*, 1973, 1977; *Wasson*, 1967, 1969, 1970, 1990, 1999; *Wasson and Canut de Bon*, 1998; *Wasson and Choi*, 2003; *Wasson and Kallemeyn*, 2002; *Wasson and Richardson*, 2001; *Wasson and Schaudy*, 1971; *Wasson and Wang*, 1986; *Wasson et al.*, 1980, 1988, 1989, 1998].

abundance [*Gaffey*, 1976; *Britt and Pieters*, 1987]. Mössbauer spectra of both the "as is" and the brushed surface show ~5% of the Fe in the ferric state. The brushed meteorite surface is enriched in P, S and Cl when compared to Martian soil (R. Gellert et al., manuscript in preparation, 2008). The coating may be a remnant of a fusion crust; some of the Fe may have been oxidized during the meteorite's descent through the Martian atmosphere. Preferential melting of mineral inclusions such as schreibersite and troilite would have led to the deposition of P and S, and the formation of the ablation features. On the other hand, it is not clear whether in a thin, oxygen-poor atmosphere an oxidized fusion crust would have formed at all. On Earth, weathering may proceed by the introduction of Cl into the

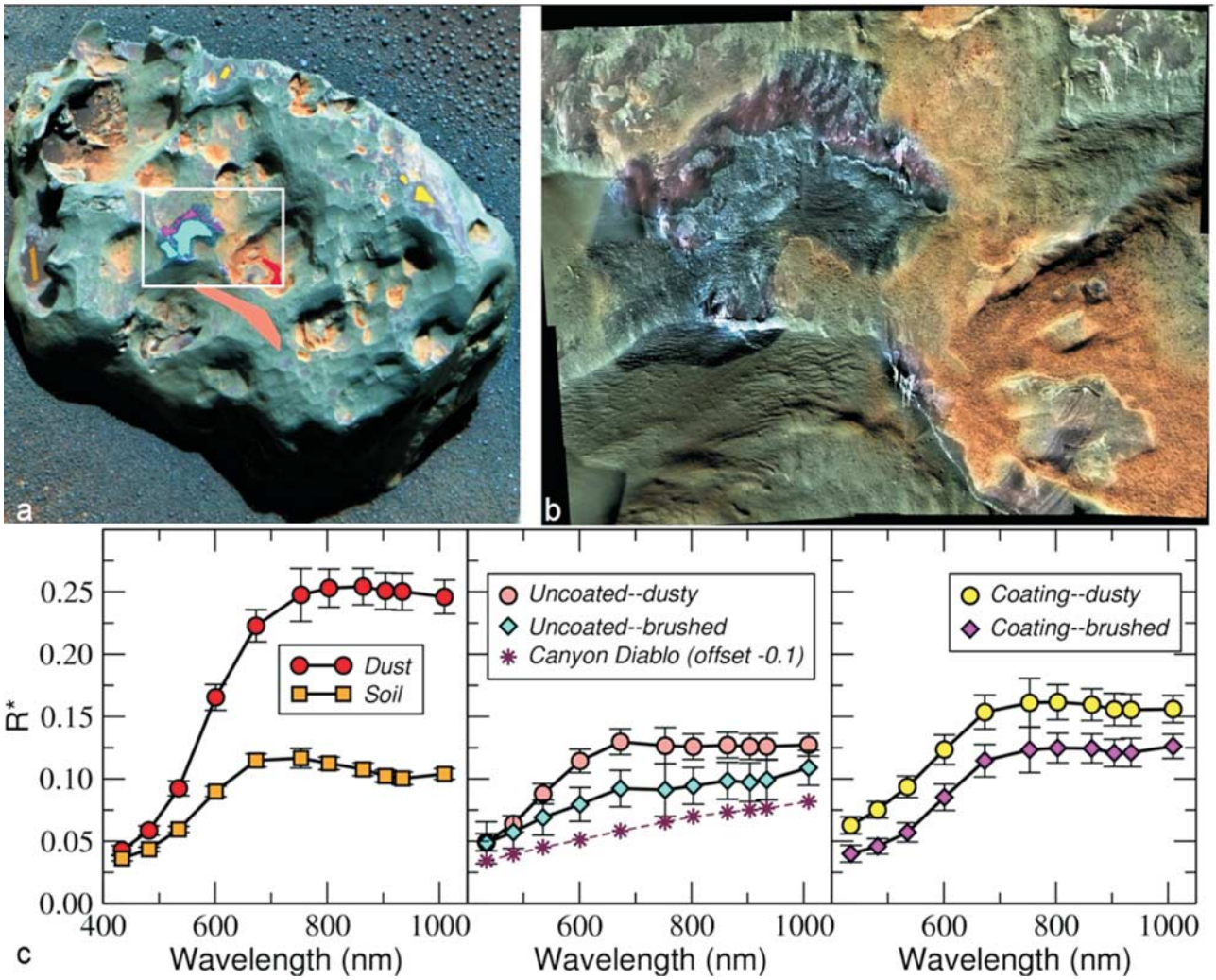

Figure 4. (a) Pancam false-color image (sol 352, P2596) of Heat Shield Rock created from 753 nm, 535 nm, and 432 nm images. White box outlines region of Microscopic Imager mosaic acquired after RAT brush (sol 349), shown in Figure 4b, with color overlain from the same Pancam false-color images as in Figure 4a. Bright streaks are caused by image saturation in the MI mosaic. Colored regions in Figure 4a are regions of interest from which Pancam spectra were extracted as shown in Figure 4c. Canyon Diablo laboratory spectrum (RELAB MI-CMP-008, spectrum 001) is vertically offset −0.1.

rock [*Buchwald and Clarke*, 1989]. Chlorine is ubiquitously present in Martian fines at much higher levels compared to terrestrial soils [e.g., *Clark et al.*, 1982; *Yen et al.*, 2005]. Oxidation of the Fe in the presence of Cl leads to the formation of akaganeite, β-FeOOH, which is one of several iron oxides whose Mössbauer parameters could be reconciled with the data for the nanophase ferric oxide component. Each instrument's field of view contained both coated and uncoated material, and therefore any assignment of these features to either the rock or the coating is equivocal.

[15] MiniTES spectra lack obvious features that can be attributed to Fe oxides. This implies that the dust cover that has been removed through RAT-brushing is relatively thin ($< \sim 30-50$ μm), and any coating is only a minor component of the total surface area. Mini-TES has a larger field of view than the other instruments and so did not observe in isolation any of the coating. The coating does not cover the whole meteorite surface but rather occurs in isolated patches (Figures 2c and 4). This can be interpreted in several ways: (1) the meteorite is a relatively recent arrival on the Meridiani plains with insufficient time for alteration of the complete surface to have occurred; (2) alteration of the complete surface has occurred but the evidence for it has been stripped off the rock through the action of wind; (3) the meteorite arrived on the plains early in their history, but alteration has been so inefficient that the rock has remained relatively pristine over the duration of its presence on the plains; or (4) the rock could have been partially buried at different times, and the coating may have formed when only that portion of the rock was above the soil level.

3. Barberton

[16] On sol 121 of its mission, Opportunity started to investigate the ~3 cm-sized pebble Barberton at the rim of Endurance crater (Figure 5). The pebble was analyzed in

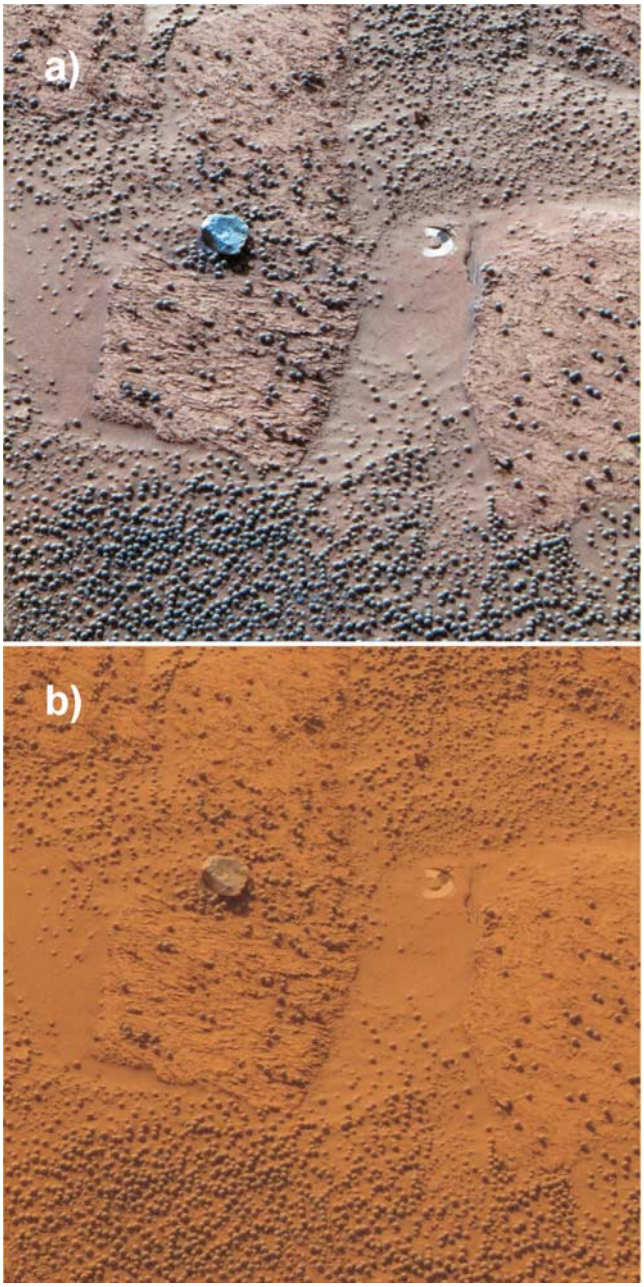

Figure 5. The ~3 cm cobble Barberton at the rim of Endurance crater, (a) in a false color Pancam image highlighting the differences between the hematite spherule lag deposit, sulfate-rich outcrop, and basaltic soil (http://marswatch.astro.cornell.edu/pancam_instrument/images/False/Sol123B_P2535_1_False_L257.jpg); (b) an approximate true color Pancam image showing the omnipresent dust as a red hue (http://marswatch.astro.cornell.edu/pancam_instrument/images/True/Sol123B_P2535_1_True_RAD.jpg). The circular depression from the Mössbauer contact plate indicates the soil target McDonnell_HillTop_Wilson.

situ by the MI (Figure 6), the APXS, and the MB spectrometer. Owing to mission constraints, integration times for both spectrometers were limited. Barberton was too small to be brushed or abraded with the RAT. A neighboring soil target, McDonnell HillTop Wilson (Figure 5), was investigated with the APXS and MB instruments for comparative studies.

3.1. Chemistry

[17] Table 1 shows the chemical composition of Barberton compared to the soil target McDonnell HillTop Wilson which has a composition similar to the most dusty of the basaltic soils found throughout Opportunity's traverse. Barberton stands out by its high Mg and Ni contents. The Mg content is the highest at Meridiani Planum, approximately twice that of basaltic soils or rock fragments of basaltic composition such as Bounce Rock. It is, however, lower than rocks of ultramafic composition

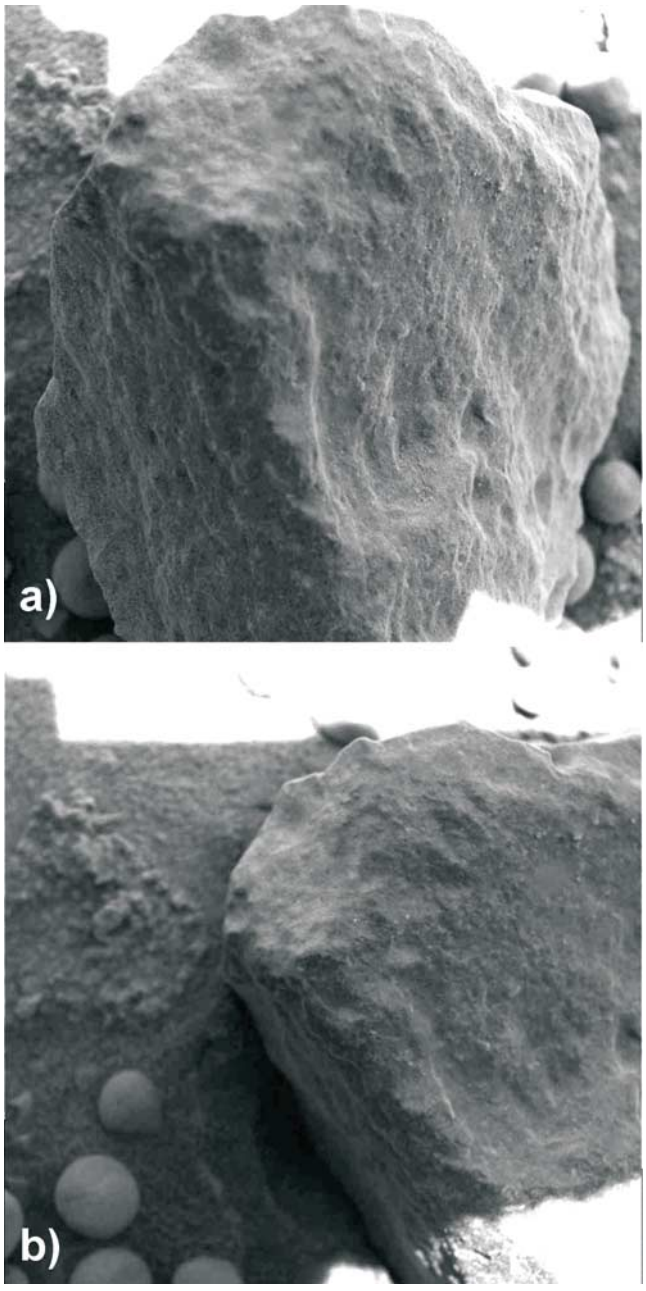

Figure 6. Microscopic Imager pictures of Barberton (sol 121, sequence ID p2956). Each frame is 31 mm square.

Table 1. Chemical Composition of Barberton, Santa Catarina and Related Targets

			Barberton Minus Percentage of Soil				
	Sol B122	Sol B123	25%	35%	Sol B1046	Sol A688	Sol A700
Feature	FigTree	HillTop_Wilson				Algonquin	Commanche
Target	Barberton2[b] cobble	McDonnell[b] soil			Santa Catarina[b] cobble	Iroquet_brushed rock (Gusev)	Palomino rock (Gusev)
			Weight Percent				
Na_2O	1.76	2.38	1.55	1.43	1.51	1.59	1.12
MgO	14.79	7.61	17.18	18.66	18.04	22.3	24.75
Al_2O_3	6.2	9.21	5.20	4.58	4.35	4	2.93
SiO_2	44.3	45.3	43.97	43.76	44	40.6	41.3
P_2O_5	0.66	0.87	0.59	0.55	0.61	0.63	0.45
SO_3	5.56	7.12	5.04	4.72	5.09	4.32	2.69
Cl	0.6	0.84	0.52	0.47	0.62	0.87	0.61
K_2O	0.29	0.51	0.22	0.17	0.14	0.12	0.04
CaO	4.42	6.73	3.65	3.18	3.43	2.61	1.93
TiO_2	0.51	0.97	0.36	0.26	0.24	0.35	0.25
Cr_2O_3	0.5	0.36	0.55	0.58	0.61	0.87	0.71
MnO	0.36	0.37	0.36	0.35	0.38	0.38	0.43
FeO	18	12.5	19.83	20.96	20.6	21.2	22.6
Fe_2O_3[a]	1.98	5.66	0.75	0.00			
			Parts per Million				
Ni	1639	503	2018	2251	3207	891	1000
Zn	207	376	151	116	164	131	132
Br	47	35	51	53	59	72	156
SO3/Cl	9.27	8.48	9.69	10.04	8.21	4.97	4.41

[a] Fe^{3+}/Fe_T ratios from MB have not been taken into account for targets Santa Catarina, Iroquet_brushed, and Palomino. For these targets, FeO represents the total Fe content.
[b] Values from R. Gellert et al. (manuscript in preparation, 2008).

investigated in the Columbia Hills in Gusev Crater by the Spirit rover [*Mittlefehldt et al.*, 2006]. The Ni content is exceeded at Meridiani Planum only when compared to Santa Catarina and Heat Shield Rock. High Ni may indicate a meteoritic origin. On the other hand, the Ni content of olivine crystals in rocks of ultramafic composition can be very high. Alternatively, the chemical composition of Independence class rocks investigated by Spirit in Gusev Crater suggests they have been altered to montmorillonite or its compositional equivalent [*Clark et al.*, 2007], a process during which Ni could have been mobilized and accumulated [*Yen et al.*, 2006]. Rocks of the Independence class investigated by Spirit in the Columbia Hills have variable Ni contents. The upper limit of that range, 2068 ppm, exceeds the Ni content of Barberton. The high Ni target of Independence class could also be a breccia incorporating Ni-rich meteoritic infall material [*Clark et al.*, 2007].

[18] Barberton did not completely fill the field of view of the APXS instrument and a contribution from the surrounding material must be taken into account in determining its composition. We subtracted certain percentages of the composition of the soil target McDonnell HillTop Wilson in an attempt to compensate for that contribution (Table 1). For this comparison of Barberton and McDonnell HillTop Wilson, based on Mössbauer measurements of iron oxidation state [*Morris et al.*, 2006], the total Fe contents have been divided into divalent and trivalent iron listed as FeO and Fe_2O_3, respectively. The maximum contribution of the soil is reached when for one of the elements the fraction of soil times the abundance of the element in the soil equals the abundance of that element in the Barberton measurement. This is the case for Fe_2O_3 at a subtraction of 35% soil. Because the bulk composition of Barberton likely contains less Fe_2O_3 than indicated by the surface measurement given in Table 1 (see also discussion of Mössbauer results below), the value of 35% is taken as the upper limit of contribution of surrounding material. The subtraction of up to 35% of a soil component leads to a composition rich in Mg and Ni and poor in Al and Ca unlike any other material analyzed by Opportunity except for Santa Catarina (see below). Note that the differing APXS and MB sampling depths could complicate this interpretation, as Fe oxidation state is determined over a greater depth than the elemental chemistry.

[19] The amount of S in Barberton is relatively high. On the one hand, the high S might be attributed to a weathering rind or adhering dust on the rock surface. Fines may have been welded or sintered onto Barberton upon impact [e.g., *Hörz and Cintala*, 1984]. The elements S and Cl are correlated in basaltic soils at Meridiani, and the SO_3/Cl ratio in the Barberton measurement falls within that range. However, the ratio increases after the measured composition is corrected for soil in the analysis, suggesting that some of the S is inherent to Barberton and that it could be present as reduced S, i.e., in the form of troilite.

3.2. Mineralogy

[20] The Fe-bearing mineralogy determined by Opportunity's Mössbauer spectrometer is dominated by Fe^{2+} in the minerals olivine (51%) and pyroxene (32%) [*Morris et al.*, 2006]. In addition, the spectrum shows contributions from nanophase ferric oxides (6%) and metallic Fe

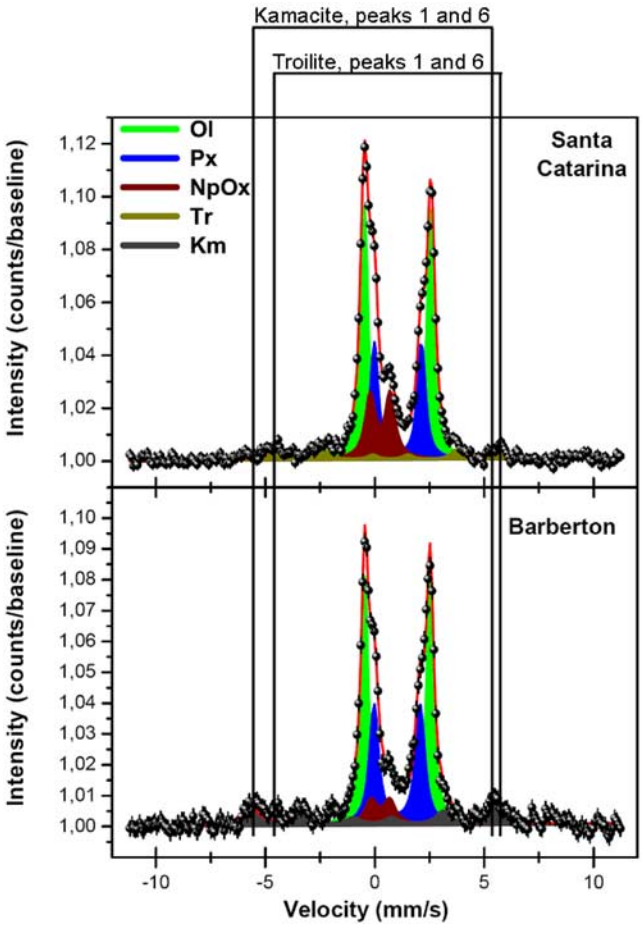

Figure 7. Mössbauer spectra of (top) Santa Catarina and (bottom) Barberton. Peaks 1 and 6 of the magnetically split sextets typical for kamacite and troilite are indicated. Troilite in Barberton and kamacite in Santa Catarina are, if present, hard to resolve against the statistical background. Ol, olivine; Px, pyroxene; NpOx, nanophase ferric oxides; Tr, troilite; Km, kamacite.

in the form of kamacite (11%), an Fe-Ni alloy (Figure 7). The numbers given in brackets are Mössbauer subspectral areas [*Morris et al.*, 2006] and represent the percentage of total Fe associated with the respective mineral. *McSween et al.* [2008], for example, discuss how to reconcile the data with mineralogical information from APXS and Mini-TES. The range of Fe oxidation states suggests the presence of a fusion crust, fines welded onto Barberton upon impact, and/or a weathering rind. Weathering products may include Ni-rich Mg-sulfates and "metallic rust" rich in Fe, Ni, and S, such as identified as terrestrial weathering products in meteorites collected in Antarctica [*Gooding*, 1984, 1986]. The latter may contribute to the nanophase ferric oxide phase identified in the Mössbauer spectrum of Barberton.

[21] Barberton may contain some troilite, FeS, depending on the amount of sulfur present in its bulk composition. Using a model that included a troilite component to fit the Barberton Mössbauer spectrum yielded ~2% of the Fe in troilite. However, the quality of the fit did not improve significantly, and hence evidence for troilite in the Mössbauer data is inconclusive.

3.3. Classification

[22] Although unique among samples investigated at Meridiani Planum, the chemical composition of Barberton, rich in Mg and Ni and poor in Al and Ca, would be consistent with an ultramafic rock of Martian origin. Kamacite or metallic Fe have not been identified in any rock on Mars, other than the iron meteorite Heat Shield Rock, nor in any of the Martian meteorites in collections on Earth. However, the most reduced among the Martian meteorites, QUE94201, crystallized slightly above the iron-wüstite buffer [*McKay et al.*, 2003; *Karner et al.*, 2007], and an occurrence of metallic Fe in Martian crustal or mantle material cannot be excluded.

[23] When compared to a range of meteorites [*Nittler et al.*, 2004], Barberton is similar in Mg/Si, Ca/Si and Al/Si ratios to howardites and diogenites, but enriched in S/Si, Fe/Si and Ni (Figure 8). Mesosiderites provide a better match because they have a howardite-like silicate composition with additional metal and sulfide. Assuming a silicate clast of howardite-like composition, e.g., the howardite Bununu [*Jarosewich*, 1990], and adding small amounts of metal ($Fe_{90}Ni_{10}$) and sulfide (FeS), the Barberton composition can be reproduced (Table 2).

[24] Mesosiderites typically do not contain abundant olivine, although centimeter-sized olivine clasts have been observed in several mesosiderites [*Boesenberg et al.*, 1997; *Delaney et al.*, 1980; *McCall*, 1966; *Mittlefehldt*, 1980; *Nehru et al.*, 1980]. However, the modal abundance of olivine is typically much less than that of pyroxene in mesosiderites [*Powell*, 1970; *Prinz et al.*, 1980]. A thin section of the meteorite MIL03443 shows a groundmass of coarse comminuted olivine and has been tentatively classified as a clast from a mesosiderite [*McCoy*, 2006].

[25] *Kimura et al.* [1991] investigated enclaves in the Vaca Muerta mesosiderite. Modal abundances of metal determined for several clasts and the whole enclave of an olivine-orthopyroxenite monomict breccia range from trace amounts to 7.1 vol %. Calculating the modal amount of metal with soil-subtracted Barberton values yields 1.7 to 1.9 vol %, whereby we used the simplifying assumptions that all Ni is in kamacite and that kamacite is $[Fe_{0.95},Ni_{0.05}]$. On the basis of the chemical similarity to mesosiderite silicate clasts and its metal content we favor a meteoritic origin for Barberton. It may be the first stony meteorite discovered on the surface of Mars.

4. Santa Catarina

[26] A field of cobbles extending over an area of 96 by 108 m as visible from the rover was encountered while traversing the Cabo Anonimo promontory on the rim of Victoria crater between sols 1034 and 1055. The first of these cobbles examined, named Santa Catarina, measures about 14 cm in its longest dimension and about 11 cm across. It received the full complement of IDD instrument analyses. The rock could not be abraded or brushed because of its geometry. APXS, Mössbauer, and MI measurements were done on an "as is" but relatively dust-free surface (Figure 9). As described below, the results suggest a

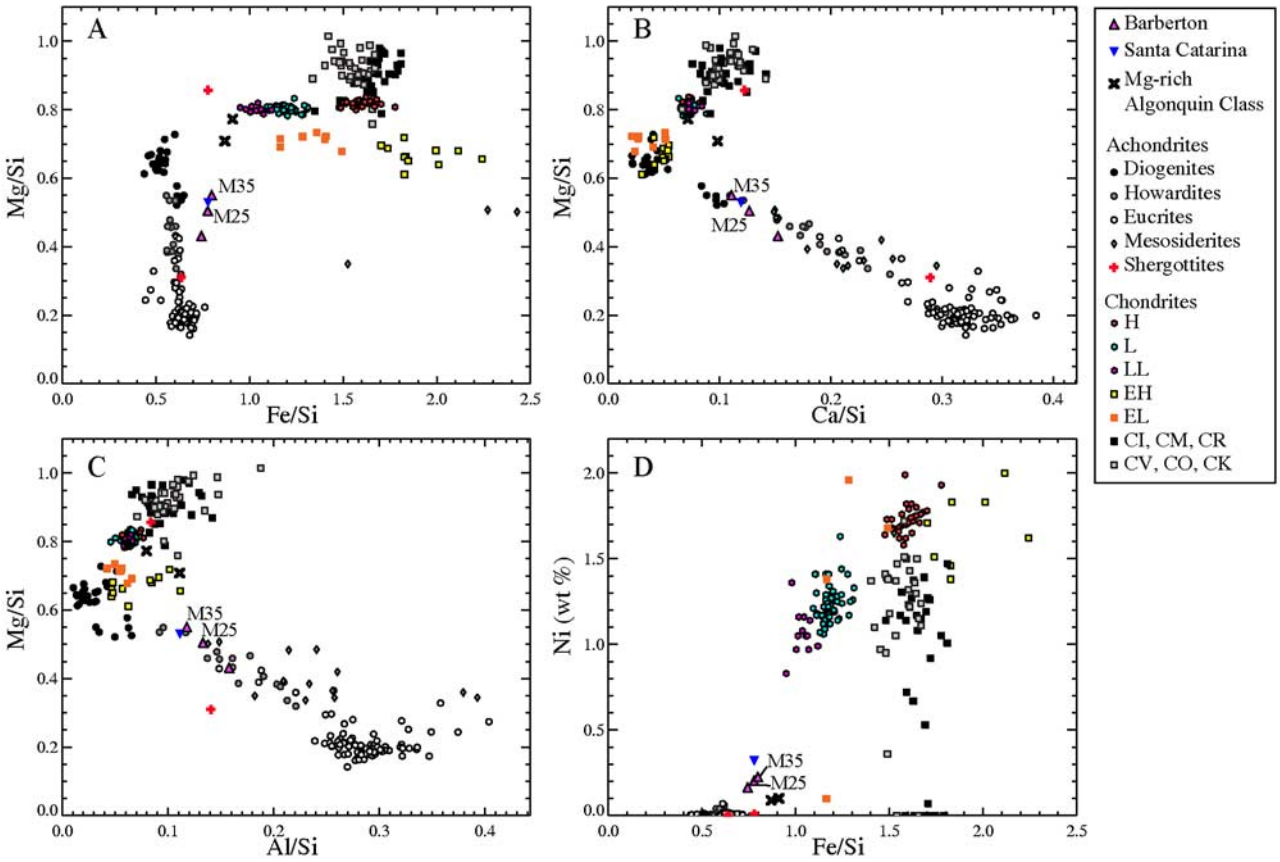

Figure 8. Element ratio plots comparing Barberton, Santa Catarina, and two Mg-rich ultramafic rock targets of the Algonquin class investigated by Spirit in Gusev Crater to several classes of meteorites, in particular, chondrites and HEDs. The areas in which mesosiderites plot with increasing metal/silicate ratio are indicated where applicable.

possible genetic link to Barberton. Mini-TES data were acquired for Santa Catarina on sol 1055. Seventeen additional nearby rocks were targeted for remote sensing using Mini-TES in this cobble field: Mafra, Lajes, Xaxim, Videira, Joacaba, Tubarao, Igreja, Florianopolis, Gallego, Vasco, Gomes, Santandres, Deseado, Narrows, Sardines, Trabajo, and Paloma. After background subtraction and using the current model to correct for dust on the Mini-TES pointing mirror, spectra from this suite of rocks indicate little variation among them. Pancam spectra reveal two different spectral types within the cobble field: One with a broad NIR absorption with an apparent band minimum at 1009 nm, and one with a narrower NIR absorption with a 934 nm band minimum and a distinct 864 to 904 nm downturn (only the latter is shown in Figure 10). However, the differences may be a consequence of sampling because only a few pixels per cobble were averaged. For example, the sampling might have preferentially hit olivine phenocrysts on some and orthopyroxene on others. It is therefore possible that Santa Catarina represents the chemical, textural, and mineralogical nature of this group.

4.1. Texture and Morphology

[27] Santa Catarina is a brecciated rock containing some clasts with possible igneous quench textures. Figure 11 shows an MI mosaic of Santa Catarina obtained on sol 1045. Fractures are clearly visible in the rock, as are several clasts. One clast appears to consist of light-toned crystals in a darker matrix. Another clast reveals what might be an igneous quench texture of olivine phenocrysts.

4.2. Chemistry

[28] Santa Catarina has an ultramafic composition with unusually high Ni. Compared to other Meridiani Planum materials, sulfate-rich outcrop, basaltic soil, Barberton, and other, nonmeteoritic rock fragments, Santa Catarina is most similar to Barberton. Ratios of Mg/Si, Ca/Si, Al/Si, S/Si, Fe/Si are all very close to soil-subtracted Barberton values (Figure 8). Ultramafic rocks investigated by Spirit in Gusev Crater also have a similar chemical composition in some

Table 2. Model Calculation of a Mix of Howardite Material Mixed With (Fe,Ni) and FeS Compared to Barberton

	Fe	Ni	S	Si	Component,%
Howardite[a]	14.1	0.06	0.35	22.7	0.94
Fe90Ni10	90	10	0	0	0.015
FeS	63.5	0	36.5	0	0.045
Mix	17.45	0.21	1.97	21.35	
Barberton - 35% soil	16.33	0.23	1.89	20.45	
	Mix	Barberton			
Fe/Si	0.82	0.80			
Ni	0.21	0.23			
S/Si	0.09	0.09			

[a]Howardite composition of Bununu from *Jarosewich* [1990].

Figure 9. Pancam approximately true color image of Santa Catarina. In the image, the lower, dark-toned area of the rock appears to be relatively dust-free and was investigated by MI (see Figure 10), APXS, and MB. Santa Catarina measures approximately 14 cm in length and 11 cm across (http://marswatch.astro.cornell.edu/pancam_instrument/images/True/Sol1055B_P2564_1_True_RAD.jpg).

respects, in particular the Algonquin class rock targets Algonquin Iroquet Brushed and Comanche Palomino (Table 1). However, these Algonquin class rocks have higher Mg and lower Si than either Santa Catarina or Barberton. The Ni content of Santa Catarina is more than three times the highest value for Algonquin class (1000 ppm). The investigated surface appeared to be relatively free of dust and no attempt for a dust correction was made.

[29] Because of the similarity of the APXS composition of Santa Catarina and the soil-corrected composition of Barberton, and because the MI images of Barberton show dust adhering to the analyzed surface, we have done additional compositional modeling [e.g., *Jolliff et al.*, 2007] to test whether a thin layer of dust might make the derived composition of Barberton approach the composition of Santa Catarina. We consider the effect of a thin layer of dust primarily through the attenuation of low-energy X rays compared to high-energy X rays. Attenuation coefficients were calculated from the average attenuation cross sections for the characteristic X-ray lines of measured elements, taken from *Gellert et al.* [2006, Table 1]. The compositions of the soil targets McDonnell HillTop Wilson and Les Hauches were selected for this analysis because they have the most dust-like visible and Mössbauer spectral characteristics, for example, high nanophase ferric oxide contents [*Morris et al.*, 2006]. Attenuation factors are calculated using the absorption equation, $I = I_0 e^{-\mu x}$, recast as $I/I_0 = e^{-\mu x}$, where μ is the attenuation coefficient and x is the layer thickness, expressed in mg/cm^2.

[30] The primary effect of thin layer dust coatings (Figure 12) is to make the light element concentrations more dust-like and less like the substrate (in this case, Barberton). X rays from heavy elements, on the other hand, are less attenuated by the dust layer and thus reflect more the character of the substrate. Figure 12 shows that a thin layer dust coating on Barberton is not consistent with a rock (substrate) composition similar to Santa Catarina. However, a simple two-component (rock-soil) mixing model used to calculate the composition of Barberton, is consistent for the rock-forming elements with a Santa Catarina-like composition for Barberton, with 25–35% soil contamination in the APXS analysis.

4.3. Mineralogy

[31] The Fe-bearing mineralogy is, as in Barberton, dominated by Fe^{2+} in the minerals olivine (52%) and pyroxene (26%). Santa Catarina is more oxidized than Barberton with 14% of the Fe as nanophase ferric oxide. Contrary to Barberton, troilite (7%) is identified in the MB spectrum of Santa Catarina whereas there is no conclusive evidence for kamacite within the available statistics (Figure 7). Fitting models containing kamacite put it at or below the detection limit of 2% without improving the quality of the fit significantly, which is unexpected considering the high Ni content of the rock. It is also possible that the brecciated structure of Santa Catarina is responsible for mineralogical heterogeneity larger than the field of view of the Mössbauer instrument.

4.4. Classification

[32] We do not attempt to classify Santa Catarina as any known meteorite type because the unidentified mineralogical host of the Ni leaves room for a Martian origin of the rock. Rather than in kamacite, the Ni may reside in taenite or tetrataenite leaving the amount of Fe associated with that phase at or below MB detection limits. On the other hand, Ni may reside in the olivine phase. In this case, the lack of metallic iron would make a Martian origin of Santa Catarina more likely.

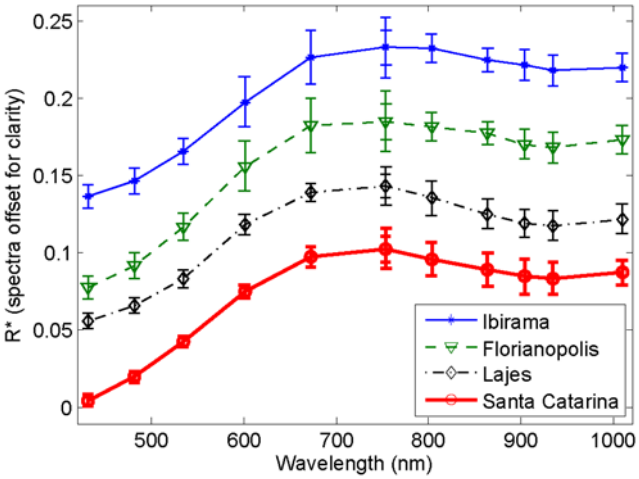

Figure 10. Pancam spectra of several specimens in the Santa Catarina cobble field are very similar to the spectrum of Santa Catarina itself.

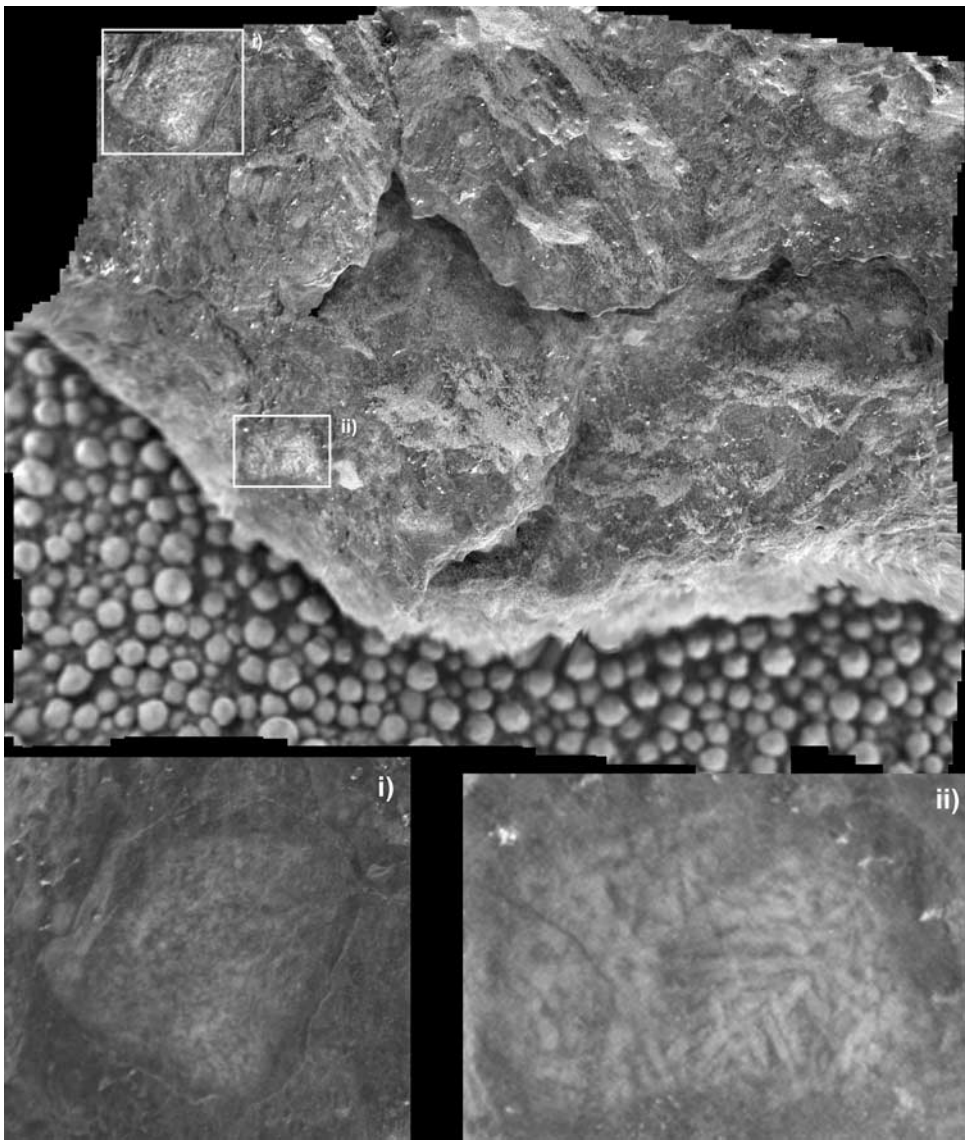

Figure 11. Mosaic of radiometrically calibrated MI images of Santa Catarina, using a digital elevation model. The single frames were acquired on Sol 1045 while the target was fully shadowed. The image is about 5 cm high. The APXS with a circular field of view of ~3 cm when in contact and the MB with a field of view of ~1.4 cm when in contact measured the area in the center of the mosaic. Subsets show image i, a clast consisting of light-toned crystals in a darker matrix; and image ii, a clast revealing what might be an igneous quench texture of olivine phenocrysts.

[33] Troilite has also been observed in Martian meteorites [e.g., *Floran et al.*, 1978], but it is only a trace phase. Troilite is prevalent in mesosiderites [e.g., *Mittlefehldt et al.*, 1998, and references therein], and is more abundant than metal in the enclaves of the Vaca Muerta mesosiderite investigated by *Kimura et al.* [1991]. Therefore it is possible that some troilite remained while the metal phase was completely altered to, e.g., Ni-rich Mg sulfates and "metallic rust." These phases have been described as terrestrial weathering products in meteorites collected in Antarctica [*Gooding*, 1984, 1986]. Compared to Barberton, Mössbauer spectra of Santa Catarina show a higher percentage of Fe in the nanophase ferric oxide phase.

[34] Santa Catarina could also conceivably be a breccia of Martian materials excavated from deep within Victoria crater mixed with material from the projectile that formed the crater. On the basis of its overall similarity to Barberton and its high Ni content, we favor a meteoritic origin for Santa Catarina. Barberton, Santa Catarina and adjacent cobbles together may represent a meteorite strewn field.

5. Other Possible Meteorites

[35] There are likely many more meteorites among the cobbles and float rocks which Opportunity passed during the traverse across the Meridiani plains. While iron meteorites may be identified with a high degree of certainty by remote sensing alone, only an investigation with the full suite of the Athena science package can yield a positive identification of stony meteorites. An attempt at classifica-

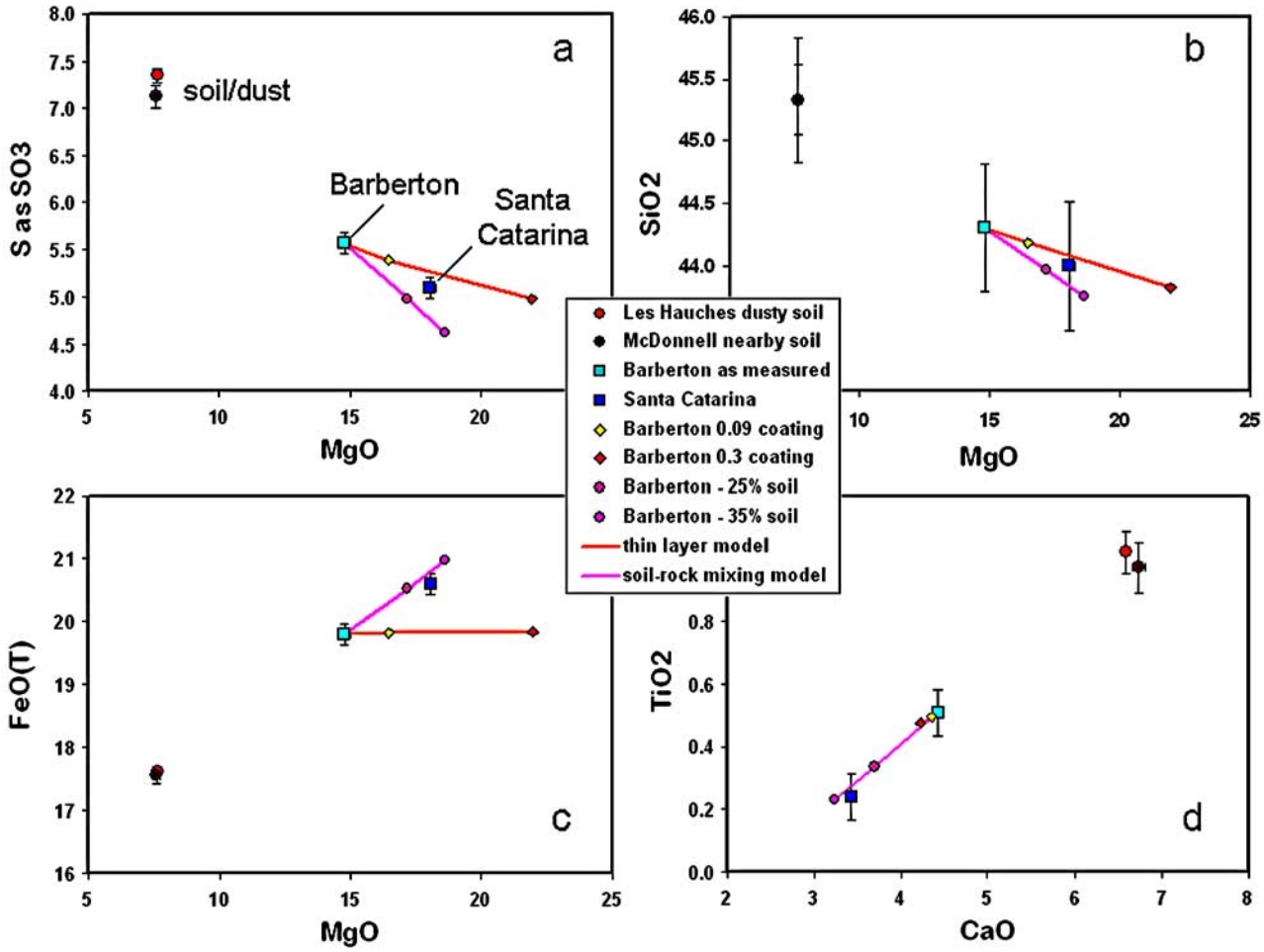

Figure 12. Compositional plots showing models of the Barberton measured composition as a mixture of rock and soil vs. rock with a thin coating of dust/soil. Error bars reflect analytical uncertainties based on counting statistics. Dust/soil is modeled using two different compositions: (1) Les Hauches bright soil and (2) McDonnell HillTop Wilson soil (adjacent to Barberton). For the elements plotted here, these compositions are very similar. Les Hauches has the highest concentration of nanophase ferric oxide as measured by the Mössbauer spectrometer, suggesting that it is the best available proxy for the dust bulk composition and is therefore used in the calculations. The rock-soil mixing model uses simple linear mixing. The thin layer model uses X-ray transmission coefficients to model the Barberton composition as a thin layer of soil/dust coating the rock, with layer thickness (0.09 and 0.3) in mg/cm^2 (see text). (a) MgO versus SO_3 and (b) MgO versus SiO_2 suggest that the two models bracket the composition of Santa Catarina. However, (c) MgO versus FeO(T) and (d) CaO versus TiO_2 indicate that the soil-rock mixing model accounts for most of the compositional differences between Barberton and Santa Catarina, whereas the thin layer model does not. The model results indicate that if Barberton and Santa Catarina in fact have similar compositions, simple soil subtraction provides a better explanation for nearly all elements than does the thin layer model. Soil subtraction consistently gives a solution between 25% and 35% soil to match the Santa Catarina composition.

tion of meteorites is also possible only with data from the full science package. Most rock fragments have been investigated with the remote sensing instruments only. Several meteorite candidates can be identified among them.

[36] A grouping of cobbles was observed at the rim of Endurance crater on sol 111 (Figure 13). Morphologically they appear similar to Barberton and unlike the sulfate-rich outcrop material. Figure 13b shows spectra from this grouping along with the spectrum of Barberton acquired on sol 123. Barberton shows a generally "red" spectrum in the near infrared (longward of 700 nm) with generally increasing reflectance. This is different from the sol 111 cobble spectra which are either flat or have decreasing reflectance with wavelength in the near infrared, but not significant when taking the error bars resulting from averaging several pixels on Barberton into account. Similar differences occur when Barberton is compared to Santa Catarina (Figure 13c). Thus, based on the same arguments used for the cobbles surrounding Santa Catarina, a genetic link between these cobbles and Barberton is possible.

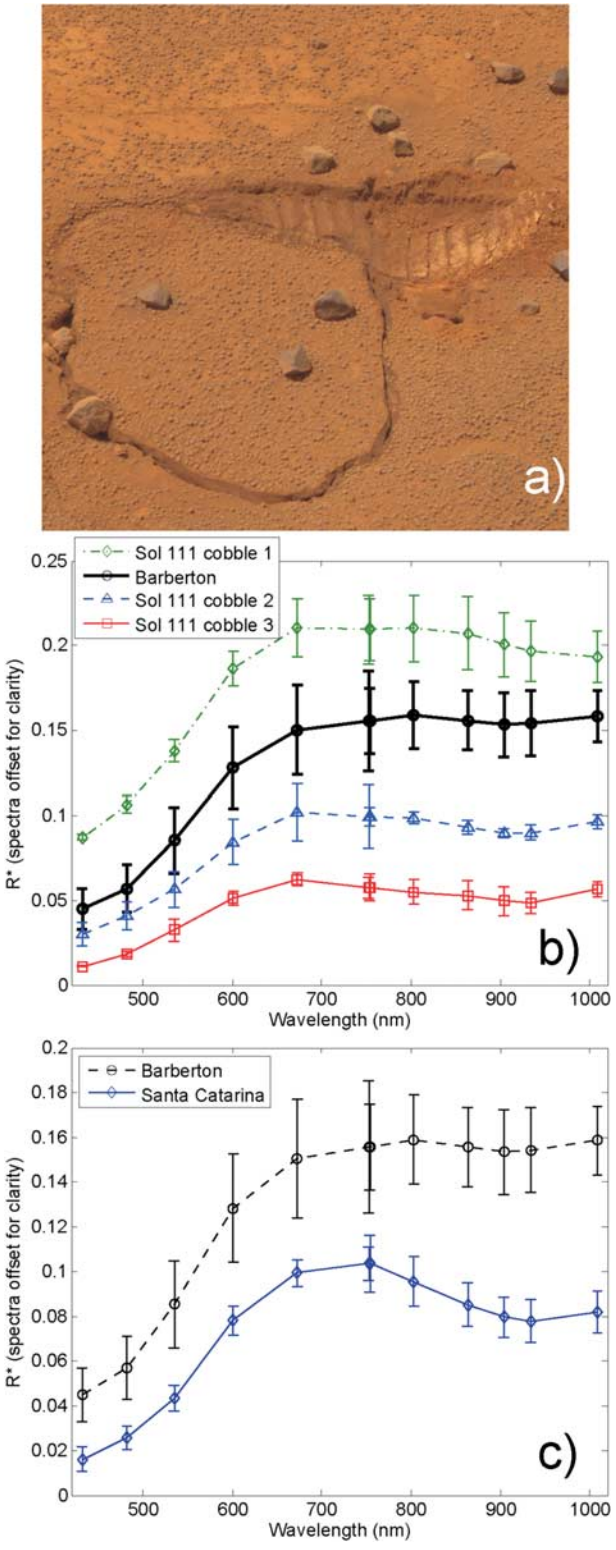

Figure 13. (a) Cobbles observed in the vicinity of Barberton at the rim of Endurance crater (http://marswatch.astro.cornell.edu/pancam_instrument/images/True/Sol111B_P2587_1_True_RAD.jpg), and (b) Pancam spectra as observed on sol 111 along with the spectrum of Barberton acquired on sol 123. Spectra have been offset for clarity; Barberton is the second spectrum from the top. (c) Comparison of Pancam spectra of Barberton and Santa Catarina.

[37] On the basis of Pancam spectral data of soil targets Aegean Crest (investigated on sol 73) and Mobarak (sols 415–417), *Weitz et al.* [2006] suggested that several clasts up to 2 cm in size might be fragments of metallic meteorites. One of these clasts was a 9 mm spherule. Metallic spherules are common on the plains surrounding Barringer Meteor Crater in Arizona, and are interpreted to be melted droplets of the Canyon Diablo iron meteorite that solidified during flight after the impact [*Blau et al.*, 1973].

[38] The presence of meteorites on Mars is of course not limited to the plains of Meridiani Planum. Because of the greater abundance of loose rocks at Spirit's landing site in Gusev Crater they are much more difficult to identify. Nonetheless, two 25 to 30 cm boulders, named Zhong Shan and Allan Hills, show pitted, spectrally gray surfaces in Pancam images and have thermal infrared characteristics in Mini-TES spectra similar to those of Heat Shield Rock (Figure 14). Unfortunately, these rocks lie on steep terrain, and because they were encountered after the failure of Spirit's right front wheel, in situ investigation was not possible.

6. General Discussion of the Data Set

6.1. Lack of Associated Impact Craters

[39] *Popova et al.* [2003] calculated that stone and iron meteoroids as small as 0.03–0.9 m (depending on strength) and 0.01 m, respectively, can reach the Martian surface at crater forming velocities (>500 m/s) under current atmospheric pressures. Craters formed by such objects would have a diameter of about 0.5–6 m and 0.3 m, respectively. *Hörz et al.* [1999] presented evidence from the Mars Pathfinder Mission for craters <1 m in diameter. Indeed, Opportunity has imaged craters in this size range (Figure 15). Chondritic meteorites impacting fines at velocities of 1.6 km/s may yield discrete pieces, whereas iron meteorites may survive velocities in excess of 2.0 km/s intact [*Hörz and Cintala*, 1984; *Bland and Smith*, 2000]. However, craters attributable to Barberton, Heat Shield Rock, or Santa Catarina as primary impactors have not been observed which leaves three possible conclusions: (1) Craters have been eroded away since impact; (2) meteorites were decelerated to near free-fall velocities prior to impact; and (3) meteorites are spalled-off fragments of an impactor.

[40] Of the three rocks in question, the iron meteorite Heat Shield Rock is the largest and strongest, potentially producing a crater of ~10 m in diameter and up to 3 m in depth [*Grant et al.*, 2006]. Craters of comparable size observed during Opportunity's traverse of the Meridiani plains show variable gradation states, ranging from fresh appearances to almost completely infilled and buried by drift [*Grant et al.*, 2006; *Golombek et al.*, 2006]. The bedrock along Opportunity's traverse consists exclusively of very soft sulfate-rich sandstone that is highly susceptible to wind erosion. Since ~0.4 Ga ago, 1–10 m of erosion and redistribution of sand at Meridiani have occurred [*Golombek et al.*, 2006]. This would have been sufficient to erase any visible trace of an impact crater formed by Heat Shield Rock.

[41] On the basis of the evidence for fluvial processes on Mars, a warmer, i.e., denser atmosphere on early Mars is

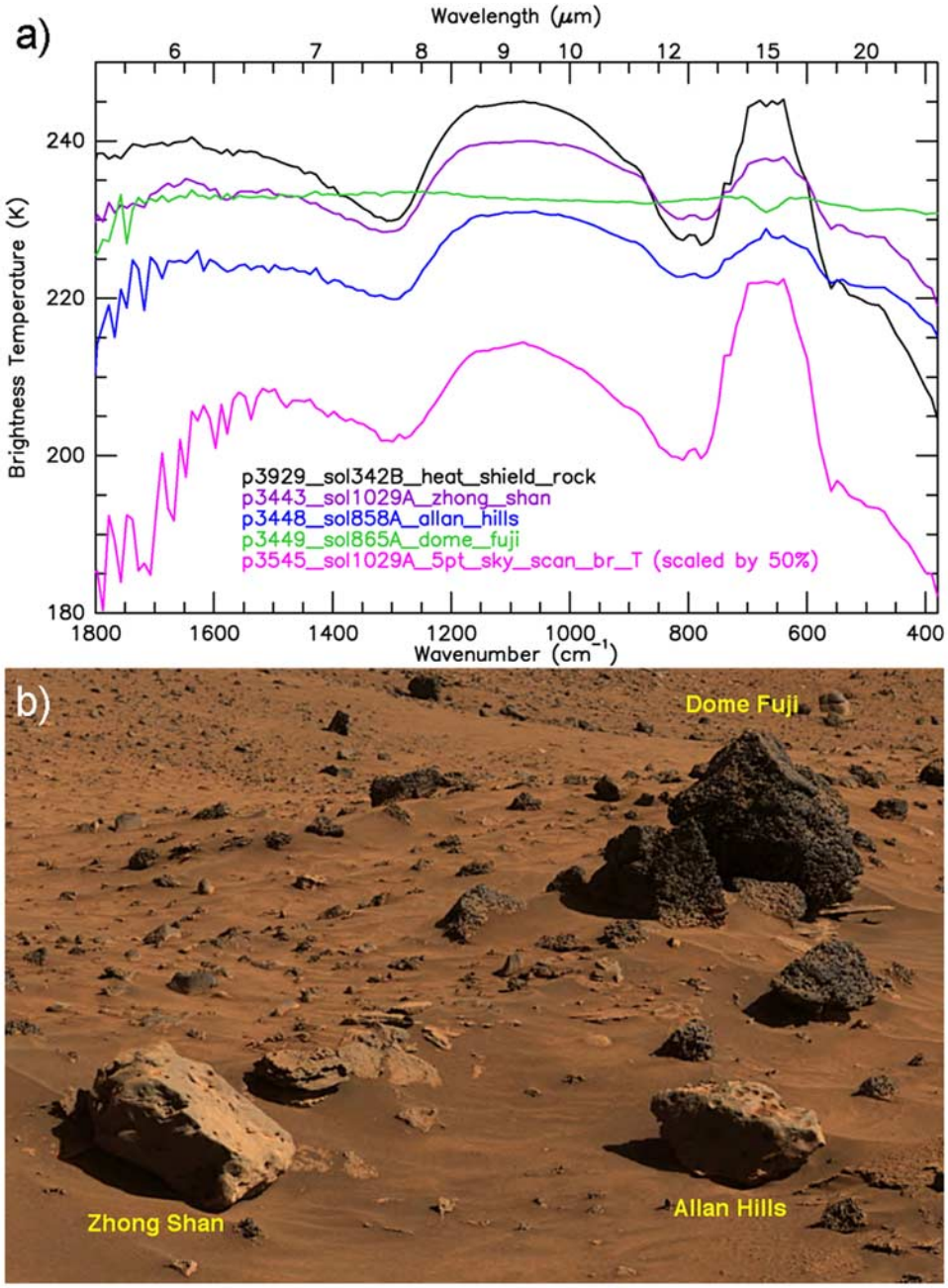

Figure 14. (a) Mini-TES and (b) Pancam observations of two probable iron meteorites in Gusev Crater. The spectrum of the known iron meteorite originally called Heat Shield rock (black) displays the spectral characteristics of the Martian atmosphere (pink) because of the highly reflective nature of metallic iron in thermal infrared wavelengths. Two other rocks called Zhong Shan (purple) and Allan Hills (blue) found in Gusev Crater by the Spirit rover have similar morphological and spectral characteristics to Heat Shield rock. A rock called Dome Fuji adjacent to the two probable iron meteorites demonstrates how different the spectrum of a basaltic rock is (green). All of the spectra are shown as brightness temperature rather than emissivity because the latter requires an accurate estimation of kinetic temperature, which is difficult for such reflective rocks.

often inferred [e.g., *Carr*, 1996]. Variations in atmospheric density on Mars may be caused by its oscillating obliquity [*Ward*, 1992] or by extensive volcanism [e.g., *Pollack et al.*, 1987]. If the Martian atmosphere were much thicker when Heat Shield Rock arrived, the meteoroid could have been decelerated to below crater forming velocity. To decelerate a rock the size of Heat Shield Rock below crater forming speeds one has to invoke a denser atmosphere, denser than 100 mbar according to *Popova et al.* [2003], at some point in the Martian past.

[42] Finally, small pieces of lightly shocked material may be spalled off from the rear of a meteorite upon impact and

Figure 15. Navcam image of two small impact craters discovered by Opportunity along her traverse across the Meridiani plains on sol 433. The largest of the two craters measures 20 cm in diameter and is 1 cm deep. The smaller of the two is 10 cm wide and less than 1 cm deep.

land distant from the primary crater with much smaller velocities relative to the surface [*Melosh*, 1989] without producing a crater. Shocked fragments of the Canyon Diablo iron meteorite, including objects the size of Heat Shield Rock, were formed in this way [*Buchwald*, 1975]. According to calculations by *Bland and Smith* [2000], only pieces of small masses between 10 to 50 g are likely to reach the Martian surface at survivable impact velocities. Whereas Barberton may fall in this mass range, Santa Catarina and Heat Shield Rock do not. Therefore, if they fell under current conditions, they are probably spalled-off fragments of larger impactors. Because Barberton was found right at the rim of Endurance crater and Santa Catarina and adjacent cobbles were found at the rim of Victoria crater, one may further speculate that they are pieces of the impactors that formed those craters. To test this hypothesis, one may look for rocks of the same composition inside the craters. If Barberton or Santa Catarina are unrelated to the formation of the craters and fell much later, a strewn field would not necessarily stop at the crater rim. Thus, finding another fragment on the floor of either Endurance or Victoria would make a strong point against this hypothesis.

6.2. Statistical Expectations Versus Identified Meteorite Types

[43] On Earth, 86% of observed meteorite falls are chondrites. Chondrites are also expected to dominate the flux on Mars. Derived from Ni abundances, *Yen et al.* [2006] estimated 1% to 3% chondritic input to soils and sedimentary rocks on Mars. Interestingly, this number coincides with the 1.5% to 2% of chondritic material on the lunar surface [*Taylor*, 1982]. But to date, no rock of chondritic chemical and mineralogical composition has been identified by either Spirit or Opportunity. The two rocks identified with most confidence as meteorites, Heat Shield Rock and Barberton, are an iron meteorite and probably a stony iron meteorite. In any case, Barberton is achondritic rather than chondritic. Achondrites and irons, in particular, generally display greater strength than chondrites and are more likely to survive impact. Taking the available MER data, i.e., the meteorite types observed and the estimated 1% to 3% chondritic input, one can speculate that chondrites are less likely than achondrites or irons to survive impact at current atmospheric conditions.

[44] Of course, the number of confidently identified meteorites is small. Neither Opportunity nor Spirit has yet conducted a systematic survey to find meteorites. Meteorites were discovered by chance, and therefore our observations are biased in certain ways. Opportunity may have been driving within a meteorite strewn field which skewed our observations. Only a small fraction of the cobbles and float rocks visible in the images documenting Opportunity's traverse have been investigated in detail. The few rocks that have been investigated in detail show that, while it is possible to identify iron meteorites with the remote sensing instruments alone with a high degree of certainty, it is much harder to differentiate rocky material and virtually impossible to distinguish between rocks of Martian and meteoritic origin from a distance. With increasing distance from the rover, cobbles fill a smaller portion of the field of view of the Mini-TES instrument. Background subtractions leave less spectral details for mineralogical interpretation with decreasing size. Also, cobbles that were investigated with the full payload were above a certain size, to allow for RAT brushing and to fill the field of view of all instruments, with Barberton being the smallest by far. *Bland and Smith* [2000] estimated that pieces of chondritic material in the range of 10–50 g could survive intact. With an average bulk density of around 3.5 g cm^{-3} for chondrites [*Wilkison and Robinson*, 2000] such pieces may be smaller than Barberton in many cases.

[45] *Bland and Smith* [2000] also speculated that there is a real possibility for future sample return missions to blindly pick up meteoritic rather than Martian material. However, the MER results suggest that the probability to come across a meteorite is in fact small. Furthermore, a payload with capabilities similar to the MER Athena instruments can distinguish between Martian and meteoritic material.

7. Summary and Conclusions

[46] The Athena instruments can identify and, in some cases, classify meteorites. However, the example of Barberton shows that only the complementary information from all instruments is sufficient.

[47] Heat Shield Rock is classified as a IAB iron meteorite based on its chemical composition. It is officially recognized and named "Meridiani Planum." It displays isolated patches of a coating.

[48] While a Martian origin for Barberton cannot be excluded, we favor a meteoritic origin. Compared to meteorite types known, Barberton's composition is most like a mesosiderite silicate clast. It may be the first stony meteorite identified on Mars.

[49] Santa Catarina is a brecciated rock containing some clasts with possible igneous quench texture. Its chemical composition is similar to Barberton. Although it has higher Ni than Barberton, (Fe,Ni) metal was not identified. On the basis of its similarity to Barberton, we favor a meteoritic origin. Santa Catarina, its adjacent cobbles, and Barberton may be part of a meteorite strewn field.

[50] Ferric nanophase oxides were detected in Barberton, Heat Shield Rock, and Santa Catarina. However, no evidence of extant well-crystalline oxyhydroxides was detected in or on any of the meteorite candidates identified thus far at Meridiani. This is consistent with anticipated alteration intensities for the near-equatorial latitudes of Mars.

[51] If Barberton, Heat Shield Rock, and/or Santa Catarina created impact craters, they were probably erased by eolian erosion processes. Alternatively, a denser atmosphere at some point in the Martian past might have decelerated the rocks enough to prevent hypervelocity impacts. If they fell under current conditions, they are probably spalled-off fragments of larger meteoroids and did not produce impact craters. It is possible that Barberton and Santa Catarina are pieces of the impactors that formed Endurance crater and Victoria crater, respectively.

[52] Two iron meteorites were identified by Spirit's remote sensing instruments only from its Winter Haven location in the Columbia Hills inside Gusev Crater.

[53] Rocks of chondritic composition have not been detected to date. Chondrites may be generally too weak to survive impact at current atmospheric densities. However, our observations may be biased because of the MER sampling strategy.

[54] Further study of meteorites on the surface of Mars will help to gain insights into past Martian surface and atmospheric processes.

[55] **Acknowledgments.** Wei Chen produced the Opportunity traverse map. We thank Fred Hörz for helpful discussions. This manuscript benefited from reviews by Kevin Righter and Alan E. Rubin. A portion of the work described in this paper was conducted at the Jet Propulsion Laboratory, California Institute of Technology, under a contract with the National Aeronautics and Space Administration. C.S. acknowledges support by an appointment to the NASA Postdoctoral Program at the Johnson Space Center, administered by Oak Ridge Associated Universities through a contract with NASA. Funding of the Mössbauer experiment and the APXS by the German Space Agency DLR under contracts 50QM9902, 50QM0014, and 50QM0005 is acknowledged.

References

Ashley, J. W., and S. P. Wright (2004), Iron oxidation products in Martian ordinary chondrite finds as possible indicators of water exposure at Mars Exploration Rover landing sites, *Lunar Planet. Sci.*, *35*, 1750.

Bell, J. F., III, et al. (2003), Mars Exploration Rover Athena Panoramic Camera (Pancam) investigation, *J. Geophys. Res.*, *108*(E11), 8063, doi:10.1029/2003JE002070.

Bland, P. A., and T. B. Smith (2000), Meteorite accumulation on Mars, *Icarus*, *144*, 21–26.

Bland, P. A., T. B. Smith, A. J. T. Jull, F. J. Berry, A. W. R. Bevan, S. Cloudt, and C. T. Pillinger (1996), The flux of meteorites to the Earth over the last 50000 years, *Mon. Not. R. Astron. Soc.*, *283*, 551–565.

Blau, P. J., and H. J. Axon (1973), Investigation of the Canyon Diablo metallic spheroids and their relationship to the breakup of the Canyon Diablo meteorite, *J. Geophys. Res.*, *78*, 363–375.

Boesenberg, J. S., J. S. Delaney, and M. Prinz (1997), Magnesian megacrysts and matrix in the mesosiderite Lamont, *Lunar Planet. Sci.*, *37*, 1491.

Britt, D. T., and C. M. Pieters (1987), Effects of small-scale surface roughness on the bidirectional reflectance spectra of nickel-iron meteorites, *Lunar Planet. Sci.*, *18*, 131–132.

Buchwald, V. F. (1975), *Handbook of Iron Meteorites*, 1418 pp., Univ. of Calif. Press, Berkeley.

Buchwald, V. F., and R. S. Clarke Jr. (1989), Corrosion of Fe-Ni alloys by Cl-containing akaganéite (β-FeOOH): The Antarctic meteorite case, *Am. Mineral.*, *74*, 656–667.

Burr, D. M., R. J. Soare, and J. P. Emery (2005), Young (late Amazonian), near-surface, ground ice features near the equator, Athabasca Valles, Mars, *Icarus*, *178*, 56–73, doi:10.1016/j.icarus.2005.04.012.

Carr, M. H. (1996), *Water on Mars*, Oxford Univ. Press, New York, USA.

Choi, B.-G., X. Ouyang, and J. T. Wasson (1995), Classification and origin of IAB and IIICD iron meteorites, *Geochim. Cosmochim. Acta*, *59*, 593–612.

Christensen, P. R., et al. (2003), Miniature Thermal Emission Spectrometer for the Mars Exploration Rovers, *J. Geophys. Res.*, *108*(E12), 8064, doi:10.1029/2003JE002117.

Clark, B. C., A. K. Baird, R. J. Weldon, D. M. Tsusaki, L. Schnabel, and M. P. Candelaria (1982), Chemical composition of Martian fines, *J. Geophys. Res.*, *87*, 10,059–10,067.

Clark, B. C., III, et al. (2007), Evidence for montmorillonite or its compositional equivalent in Columbia Hills, Mars, *J. Geophys. Res.*, *112*, E06S01, doi:10.1029/2006JE002756.

Connolly, H. C., Jr., et al. (2006), The meteoritical bulletin, no. 90, 2006 September, *Meteorit. Planet. Sci.*, *41*(9), 1383–1418.

Delaney, J. S., and C. E. Nehru (1980), Olivine clasts from mesosiderites and howardites: Clues to the nature of achondrite parent bodies, *Proc. Lunar Planet. Sci. Conf. 11th*, 1073–1087.

Dycus, R. D. (1969), The meteorite flux at the surface of Mars, *Publ. Astron. Soc. Pac.*, *91*, 399–414.

Esbensen, K. H., V. F. Buchwald, D. J. Malvin, and J. T. Wasson (1982), Systematic compositional variations in the Cape York iron meteorite, *Geochim. Cosmochim. Acta*, *46*, 1913–1920.

Floran, R. J., M. Prinz, P. F. Hlava, K. Keil, and C. E. Nehru (1978), The Chassigny meteorite: A cumulate dunite with hydrous amphibole-bearing melt inclusions, *Geochim. Cosmochim. Acta*, *42*, 1213–1229.

Gaffey, M. J. (1976), Spectral reflectance characteristics of the meteorite classes, *J. Geophys. Res.*, *81*, 905–920.

Gellert, R., et al. (2006), Alpha Particle X-Ray Spectrometer (APXS): Results from Gusev Crater and calibration report, *J. Geophys. Res.*, *111*, E02S05, doi:10.1029/2005JE002555.

Golombek, M. P., et al. (2006), Erosion rates at the Mars Exploration Rover landing sites and long-term climate change on Mars, *J. Geophys. Res.*, *111*, E12S10, doi:10.1029/2006JE002754.

Gooding, J. L. (1984), Aqueous alteration on meteorite parent bodies: Possible role of "unfrozen" water and the Antarctic meteorite analogy, *Meteoritics*, *19*, 228–229.

Gooding, J. L. (1986), Clay-mineraloid weathering products in Antarctic meteorites, *Geochim. Cosmochim. Acta*, *50*, 2215–2223.

Gooding, J. L., R. E. Arvidson, and M. Y. Zolotov (1992), Physical and chemical weathering, in *Mars*, edited by H. H. Kieffer et al., pp. 626–651, Univ. of Ariz. Press, Tucson.

Gorevan, S. P., et al. (2003), Rock Abrasion Tool: Mars Exploration Rover mission, *J. Geophys. Res.*, *108*(E12), 8068, doi:10.1029/2003JE002061.

Grant, J. A., et al. (2006), Crater gradation in Gusev Crater and Meridiani Planum, Mars, *J. Geophys. Res.*, *111*, E02S08, doi:10.1029/2005JE002465.

Herkenhoff, K. E., et al. (2003), Athena Microscopic Imager investigation, *J. Geophys. Res.*, *108*(E12), 8065, doi:10.1029/2003JE002076.

Hörz, F., and M. J. Cintala (1984), Grain size evolution and fractionation trends in an experimental regolith, *J. Geophys. Res.*, *89*, 183–196.

Hörz, F., M. J. Cintala, W. C. Rochelle, and B. Kirk (1999), Collisionally processed rocks on Mars, *Science*, *285*, 2105–2107, doi:10.1126/science.285.5436.2105.

Jarosewich, E. (1990), Chemical analyses of meteorites: A compilation of stony and iron meteorite analyses, *Meteoritics*, *25*, 323–337.

Johnson, J. R., et al. (2006), Spectrophotometric properties of materials observed by Pancam on the Mars Exploration Rovers: 2. Opportunity, *J. Geophys. Res.*, *111*, E12S16, doi:10.1029/2006JE002762.

Jolliff, B. L., W. H. Farrand, J. R. Johnson, C. Schröder, and C. M. Weitz (2006), Origin of rocks and cobbles on the Meridiani Plains as seen by Opportunity, *Lunar Planet. Sci.*, *37*, 2401.

Jolliff, B. L., B. C. Clark, D. W. Mittlefehldt, R. Gellert, and the Athena Science Team (2007), Compositions of spherules and rock surfaces at Meridiani, in *Seventh International Conference on Mars*, Abstract 3374, Jet Propul. Lab., Pasadena, Calif.

Karner, J. M., J. J. Papike, C. K. Shearer, G. McKay, L. Le, and P. Burger (2007), Valence state partitioning of Cr and V between pyroxene-melt: Estimates of oxygen fugacity for Martian basalt QUE94201, *Am. Mineral.*, *92*, 1238–1241.

Kimura, M., Y. Ikeda, M. Ebihara, and M. Prinz (1991), New enclaves in the Vaca Muerta mesosiderite: Petrogenesis and comparison with HED meteorites, *Meteorites*, *4*, 263–306.

Klingelhöfer, G., et al. (2003), Athena MIMOS II Mössbauer spectrometer investigation, *J. Geophys. Res.*, *108*(E12), 8067, doi:10.1029/2003JE002138.

Kracher, A., J. Willis, and J. T. Wasson (1980), Chemical classification of iron meteorites-IX. A new group (IIF), revision of IAB and IIICD, and data on 57 additional irons, *Geochim. Cosmochim. Acta*, *44*, 773–787.

Krumbein, W. C., and L. L. Sloss (1963), *Stratigraphy and Sedimentation*, 2nd ed., W. H. Freeman, San Francisco, Calif.

Madsen, M. B., et al. (2003), Magnetic properties experiments on the Mars Exploration Rover Mission, *J. Geophys. Res.*, *108*(E12), 8069, doi:10.1029/2002JE002029.

Maki, J. N., et al. (2003), Mars Exploration Rover Engineering cameras, *J. Geophys. Res.*, *108*(E12), 8071, doi:10.1029/2003JE002077.

Malin, M. C., K. S. Edgett, L. V. Posiolova, S. M. McColley, and E. Z. Noe Dobrea (2006), Present-day impact cratering rate and contemporary gully activity on Mars, *Science*, *314*, 1573–1577, doi:10.1126/science.1135156.

Malvin, D. J., D. Wang, and J. T. Wasson (1984), Chemical classification of iron meteorites-X. Multielement studies of 43 irons, resolution of group IIIE from IIIAB, and evaluation of Cu as a taxonomic parameter, *Geochim. Cosmochim. Acta*, *48*, 785–804.

McCall, G. J. H. (1966), The petrology of Mount Padbury mesosiderite and its achondrite enclaves, *Mineral. Mag.*, *35*, 1029–1060.

McCoy, T. J. (2006), Thin section description of sample no. MIL 03443, *Antarct. Meteorite Newsl. 29*(2), p. 32, JSC Curator's Off., Houston, Tex.

McKay, G., L. Le, E. Koizumi, and T. Mikouchi (2003), Additional constraints on the crystallization of basaltic shergottite QUE94201, *Lunar Planet. Sci.*, *34*, 2109.

McSween, H. Y., et al. (2008), Mineralogy of volcanic rocks in Gusev Crater, Mars: Reconciling Mössbauer, Alpha Particle X-Ray Spectrometer, and Mini-Thermal Emission Spectrometer spectra, *J. Geophys. Res.*, doi:10.1029/2007JE002970, in press.

Melosh, H. J. (1989), *Impact Cratering*, Oxford Univ. Press, Oxford, U. K.

Mittlefehldt, D. W. (1980), The composition of mesosiderite olivine clasts and implications for the origin of pallasites, *Earth Planet. Sci. Lett.*, *51*, 29–40.

Mittlefehldt, D. W., T. J. McCoy, C. A. Goodrich, and A. Kracher (1998), Non-chondritic meteorites from asteroidal bodies, in *Planetary Materials*, Rev. Mineral., vol. 36, edited by J. J. Papike, pp. 4.1–4.195, Mineral. Soc. of Am., Washington, D. C.

Mittlefehldt, D. W., R. Gellert, T. McCoy, H. Y. McSween Jr., R. Li, and the Athena Science Team (2006), Possible Ni-rich mafic-ultramafic magmatic sequence in the Columbia Hills: Evidence from the Spirit rover, *Lunar Planet. Sci.*, *37*, 1505.

Morris, R. V., et al. (2006), Mössbauer mineralogy of rock, soil, and dust at Meridiani Planum, Mars: Opportunity's journey across sulfate-rich outcrop, basaltic sand and dust, and hematite lag deposits, *J. Geophys. Res.*, *111*, E12S15, doi:10.1029/2006JE002791.

Nehru, C. E., S. M. Zucker, and G. E. Harlow (1980), Olivines and olivine coronas in mesosiderites, *Geochim. Cosmochim. Acta*, *44*, 1103–1118.

Nittler, L. R., T. J. McCoy, P. E. Clark, M. E. Murphy, J. I. Trombka, and E. Jarosewich (2004), Bulk element compositions of meteorites: A guide for interpreting remote-sensing geochemical measurements of planets and asteroids, *Antarct. Meteor. Res.*, *17*, 231–251.

Pollack, J. B., J. F. Kasting, S. M. Richardson, and K. Poliakoff (1987), The case for a wet, warm climate on early Mars, *Icarus*, *71*, 203–224.

Popova, O., I. Nemtchinov, and W. K. Hartmann (2003), Bolides in the present and past Martian atmosphere and effects on cratering processes, *Meteorit. Planet. Sci.*, *38*(6), 905–925.

Powell, B. N. (1970), Petrology and chemistry of mesosiderites-II. Silicate textures and compositions and metal-silicate relationships, *Geochim. Cosmochim. Acta*, *35*, 5–34.

Prinz, M., C. E. Nehru, J. S. Delaney, and G. E. Harlow (1980), Modal studies of mesosiderites and related achondrites, including the new mesosiderite ALHA77219, *Proc. Lunar Planet. Sci. Conf. 11th*, 1055–1071.

Rasmussen, K. L., D. J. Malvin, V. F. Buchwald, and J. T. Wasson (1984), Compositional trends and cooling rates of group IVB iron meteorites, *Geochim. Cosmochim. Acta*, *48*, 805–813.

Rieder, R., R. Gellert, J. Brückner, G. Klingelhöfer, G. Dreibus, A. Yen, and S. W. Squyres (2003), The new Athena alpha particle X-ray spectrometer for the Mars Exploration Rovers, *J. Geophys. Res.*, *108*(E12), 8066, doi:10.1029/2003JE002150.

Rodionov, D., et al. (2004), Mössbauer investigation of 'Bounce rock' at Meridiani Planum on Mars–indications for the first shergottite on Mars, *Meteorit. Planet. Sci.*, *39*(8), supplement, A91.

Rodionov, D. S., G. Klingelhöfer, D. W. Ming, R. V. Morris, C. Schröder, P. A. de Souza Jr., S. W. Squyres, and A. S. Yen (2005), An iron-nickel meteorite on Meridiani Planum: Observations by MER Opportunity's Mössbauer spectrometer, *Geophys. Res. Abstr.*, *7*, 10,242.

Ruff, S. W., P. R. Christensen, T. D. Glotch, D. L. Blaney, J. E. Moersch, and M. B. Wyatt (2008), The mineralogy of Gusev Crater and Meridiani Planum derived from the Miniature Thermal Emission Spectrometers on the Spirit and Opportunity rovers, in *The Martian Surface: Composition, Mineralogy, and Physical Properties*, edited by J. F. Bell III, Cambridge Univ. Press, New York, in press.

Schaudy, R., J. T. Wasson, and V. F. Buchwald (1972), The chemical classification of iron meteorites. VI. A reinvestigation of irons with Ge concentrations lower than 1 ppm, *Icarus*, *17*, 174–192.

Scherer, P., et al. (1997), Allan Hills 88019: An Antarctic H-chondrite with a very long terrestrial age, *Meteorit. Planet. Sci.*, *32*, 769–773.

Schröder, C., et al. (2006), A stony meteorite discovered by the Mars Exploration Rover Opportunity on Merdiani Planum, Mars, *Meteorit. Planet. Sci.*, *41*, supplement, 5285.

Scott, E. R. D. (1978), Iron meteorites with low Ga and Ge concentrations-composition, structure and genetic relationships, *Geochim. Cosmochim. Acta*, *42*, 1243–1251.

Scott, E. R. D., and J. T. Wasson (1976), Chemical classification of iron meteorites-VIII. Groups IC, IIE, IIIF and 97 other irons, *Geochim. Cosmochim. Acta*, *40*, 103–115.

Scott, E. R. D., J. T. Wasson, and V. F. Buchwald (1973), The chemical classification of iron meteorites-VII. A reinvestigation of irons with Ge concentrations between 25 and 80 ppm, *Geochim. Cosmochim. Acta*, *37*, 1957–1983.

Scott, E. R. D., J. T. Wasson, and R. W. Bild (1977), Four new iron meteorite finds, *Meteoritics*, *12*(4), 425–435.

Shoemaker, E. M. (1977), Astronomically observable crater-forming projectiles, in *Impact and Explosion Cratering*, edited by D. J. Roddy, R. O. Pepin, and R. B. Merril, pp. 617–628, Pergamon, New York.

Soderblom, L. A., et al. (2004), Soils of Eagle Crater and Meridiani Planum at the Opportunity rover landing site, *Science*, *306*, 1723–1726.

Squyres, S. W., et al. (2003), Athena Mars rover science investigation, *J. Geophys. Res.*, *108*(E12), 8062, doi:10.1029/2003JE002121.

Squyres, S. W., et al. (2004), The Opportunity Rover's Athena science investigation at Meridiani Planum, Mars, *Science*, *306*, 1698–1703.

Squyres, S. W., et al. (2006a), Two years at Meridiani Planum: Results from the Opportunity rover, *Science*, *313*, 1403–1407, doi:10.1126/science.1130890.

Squyres, S. W., et al. (2006b), Overview of the Opportunity Mars Exploration Rover Mission to Meridiani Planum: Eagle Crater to Purgatory Ripple, *J. Geophys. Res.*, *111*, E12S12, doi:10.1029/2006JE002771.

Taylor, S. R. (1982), *Planetary Science: A Lunar Perspective*, 481 pp., Lunar and Planet. Sci. Inst., Houston, Tex.

Ward, W. R. (1992), Long-term orbital and spin dynamics of Mars, in *Mars*, edited by H. H. Kieffer et al., pp. 298–320, Univ. of Ariz. Press, Tucson.

Wasson, J. T. (1967), The chemical classification of iron meteorites: I. A study of iron meteorites with low concentrations of gallium and germanium, *Geochim. Cosmochim. Acta*, *31*, 161–180.

Wasson, J. T. (1969), The chemical classification of iron meteorites-III. Hexahydrites and other irons with germanium concentrations between 80 and 200 ppm, *Geochim. Cosmochim. Acta*, *33*, 859–876.

Wasson, J. T. (1970), The chemical classification of iron meteorites IV. Irons with Ge concentrations greater than 190 ppm and other meteorites associated with group I, *Icarus*, *12*, 407–423.

Wasson, J. T. (1990), Ungrouped iron meteorites in Antarctica: Origin of anomalously high abundance, *Science*, *249*, 900–902.

Wasson, J. T. (1999), Trapped melt in IIIAB irons: Solid/liquid elemental partitioning during the fractionation of the IIIAB magma, *Geochim. Cosmochim. Acta*, *63*, 2875–2889.

Wasson, J. T., and C. Canut de Bon (1998), New Chilean iron meteorites: Medium octahedrites from northern Chile are unique, *Meteorit. Planet. Sci.*, *33*, 175–179.

Wasson, J. T., and B.-G. Choi (2003), Main-group pallasites: Chemical composition, relationship to IIIAB irons, and origin, *Geochim. Cosmochim. Acta*, *67*, 3079–3096.

Wasson, J. T., and G. W. Kallemeyn (2002), The IAB iron-meteorite complex: A group, five subgroups, numerous grouplets, closely related, mainly formed by crystal segregation in rapidly cooling melts, *Geochim. Cosmochim. Acta*, *66*, 445–2473.

Wasson, J. T., and J. W. Richardson (2001), Fractionation trends among IVA iron meteorites: Contrasts with IIIAB trends, *Geochim. Cosmochim. Acta*, *65*, 951–970.

Wasson, J. T., and R. Schaudy (1971), The chemical classification of iron meteorites-V. Groups IIIC and IIID and other irons with germanium concentrations between 1 and 25 ppm, *Icarus*, *14*, 59–70.

Wasson, J. T., and J. Wang (1986), A nonmagmatic origin of group-IIE iron meteorites, *Geochim. Cosmochim. Acta*, *50*, 725–732.

Wasson, J. T., J. Willis, C. M. Wai, and A. Kracher (1980), Origin of Iron Meteorite Groups IAB and IIICD, *Z. Naturforsch.*, *35a*, 781–795.

Wasson, J. T., X. Ouyang, and D. Wang (1988), Compositional Study of a Suite of Samples from the 28-t Armanty (Xinjiang) Iron Meteorite, *Meteoritics*, *23*, 365–369.

Wasson, J. T., X. Ouyang, J. Wang, and E. Jerde (1989), Chemical classification of iron meteorites: XI. Multi-element studies of 38 new irons and the high abundance of ungrouped irons from Antarctica, *Geochim. Cosmochim. Acta*, *53*, 735–744.

Wasson, J. T., B.-G. Choi, E. A. Jerde, and F. Ulff-Møller (1998), Chemical classification of iron meteorites: XII. New members of the magmatic groups, *Geochim. Cosmochim. Acta*, *62*, 715–724.

Weitz, C. M., R. C. Anderson, J. F. Bell III, W. H. Farrand, K. E. Herkenhoff, J. R. Johnson, B. L. Jolliff, R. V. Morris, S. W. Squyres, and R. J. Sullivan (2006), Soil grain analyses at Meridiani Planum, Mars, *J. Geophys. Res.*, *111*, E12S04, doi:10.1029/2005JE002541.

Welten, K. C., C. Alderliesten, K. van der Borg, L. Lindner, T. Loeken, and L. Schultz (1997), Lewis Cliff 86360: An Antarctic L-chondrite with a terrestrial age of 2.35 million years, *Meteorit. Planet. Sci.*, *32*, 775–780.

Wilkison, S. L., and M. S. Robinson (2000), Bulk density of ordinary chondrite meteorites and implications for asteroidal internal structure, *Meteorit. Planet. Sci.*, *35*, 1203–1213.

Yen, A. S., et al. (2005), An integrated view of the chemistry and mineralogy of Martian soils, *Nature*, *436*, 49–54.

Yen, A. S., et al. (2006), Nickel on Mars: Constraints on meteoritic material at the surface, *J. Geophys. Res.*, *111*, E12S11, doi:10.1029/2006JE002797.

Zipfel, J., et al. (2004), APXS analyses of bounce rock—The first basaltic shergottite on Mars, *Meteorit. Planet. Sci.*, *39*(8), A118, supplement.

Zolensky, M. E., G. L. Wells, and H. M. Rendell (1990), The accumulation rate of meteorite falls at the Earth's surface: The view from Roosevelt County, New Mexico, *Meteoritics*, *25*, 11–17.

J. W. Ashley and S. W. Ruff, School of Earth and Space Exploration, Arizona State University, Mars Space Flight Facility, Room 106, P.O. Box 876305, Tempe, AZ 85287-6305, USA.

P. A. de Souza Jr., V & M France–CEV, 60 Route de Leval, B.P. 20149, F-59620 Aulnoye-Aymeries, France.

T. Economou, LASR, Enrico Fermi Institute, 933 E. 56th St., Chicago, IL 60637, USA.

W. H. Farrand, Space Science Institute, 4750 Walnut St., Boulder, CO 80301, USA.

I. Fleischer, G. Klingelhöfer, and D. S. Rodionov, Institut für Anorganische und Analytische Chemie, Johannes Gutenberg-Universität, Staudinger Weg 9, D-55099 Mainz, Germany.

R. Gellert, Department of Physics, University of Guelph, Guelph, ON, Canada N1G 2W1.

A. F. C. Haldemann, ESA/ESTEC HME-ME, P.O. Box 299, NL-2200 AG Noordwijk ZH, Netherlands.

K. E. Herkenhoff and J. R. Johnson, U.S. Geological Survey, Astrogeology Team, 2255 N. Gemini Drive, Flagstaff, AZ 86001, USA.

B. L. Jolliff, Department of Earth and Planetary Sciences, Washington University, Campus Box 1169, One Brookings Dr., St. Louis, MO 63130, USA.

T. J. McCoy, Department of Mineral Sciences, National Museum of Natural History, 10th and Constitution Aves., N.W., Smithsonian Institution,Washington, DC 20560-0119, USA.

D. W. Ming, Astromaterials Research and Exploration Science, Mail Code KX, NASA Johnson Space Center, 2101 NASA Parkway, Houston, TX 77058, USA.

D. W. Mittlefehldt, R. V. Morris, and C. Schröder, Astromaterials Research and Exploration Science, Mail Code KR, NASA Johnson Space Center, 2101 NASA Parkway, Houston, TX 77058, USA. (christian.schroeder-1@nasa.gov)

L. R. Nittler, Department of Terrestrial Magnetism, Carnegie Institution of Washington, 5241 Broad Branch Rd. N.W., Washington, DC 20015, USA.

S. W. Squyres, Department of Astronomy, Cornell University, 428 Space Sciences, Ithaca, NY 14853, USA.

C. Weitz, Planetary Science Institute, 1700 E. Fort Lowell Road, Suite 106, Tucson, AZ 85719, USA.

A. S. Yen, Jet Propulsion Laboratory, 4800 Oak Grove Drive, Mail Stop 183-501, Pasadena, CA 91109, USA.

J. Zipfel, Sektion Meteoritenforschung, Forschungsinstitut und Naturmuseum Senckenberg, Senckenberganlage 25, D-60325 Frankfurt am Main, Germany.